Chapter 4
Nuclear Reactions: BBN, Stars, etc

This chapter is divided into three parts:
• preliminaries: thermally averaged rates and the S-factor
• application to the pp chain
• He burning

4.1 Rates and cross sections
We want to consider the reaction

$$1(p_1) + 2(p_2) \to 1'(p_{1'}) + 2'(p_{2'})$$

where the four-momentum of particle 1 is given by p_1, etc. The rate (events/unit time in some volume V) is

$$\begin{aligned} \frac{dN}{dt} &= \int d\vec{x}\ \rho_1(p_1,\vec{x})\ \rho_2(p_2,\vec{x}) \int \frac{m_1 m_2}{E_1 E_2} |M_{fi}|^2 (2\pi)^4 \delta^4(p_{1'} + p_{2'} - p_1 - p_2) \frac{m_{1'}}{(2\pi)^3} \frac{d^3 p_{1'}}{E_{1'}} \frac{m_{2'}}{(2\pi)^3} \frac{d^3 p_{2'}}{E_{2'}} \\ &= \int d\vec{x}\ \rho_1(p_1,\vec{x})\ \rho_2(p_2,\vec{x})\ |\vec{v_1} - \vec{v_2}|\ \frac{m_1 m_2}{E_1 E_2} \sigma_{12}(p_1,p_2) \end{aligned} \tag{1}$$

where $\rho_1(p_1,\vec{x})$ is the number density of particles of type 1 with four-momentum p_1 (that is, the number of particles per unit volume). The relative velocity is defined

$$|\vec{v_1} - \vec{v_2}| = \frac{\sqrt{(p_1 \cdot p_2)^2 - m_1^2 m_2^2}}{E_1 E_2} \tag{2}$$

Suppose the densities above are constant over the volume of interest (some region within a star). Then the integral over $\vec{x}$ is simple, yielding

$$r = \text{events/unit time/unit volume} = \frac{1}{V}\frac{dN}{dt} = \frac{\rho_1 \rho_2}{1+\delta_{12}} |\vec{v}_1 - \vec{v}_2| \sigma_{12} \tag{3}$$

Note the factor of $1 + \delta_{12}$. The rate should be proportional to the number of pairs of interacting particles in the volume. If the particles are distinct, this is $\sum_{ij} \propto \rho_1 \rho_2$, but if the particles are identical, the sum over distinct pairs gives $\frac{1}{2}\sum_{ij} \propto \frac{1}{2}\rho_1 \rho_2$. Note we can also write the destruction rate per particle for particle 1 due to interactions with particles of type 2 as

$$\omega_1^{(2)} = \frac{\rho_2}{1+\delta_{12}} |\vec{v}_1 - \vec{v}_2| \sigma_{12} \tag{4}$$

which is the result one usually uses in building a reaction network. If there are multiple destruction channels, $\omega_1 = \omega_1^{(2)} + \omega_1^{(3)} + ...$ and the mean lifetime is

$$\tau_1 = \frac{1}{\omega_1^{(2)} + \omega_1^{(3)} + ...} \quad \text{or} \quad \frac{1}{\tau_1} = \frac{1}{\tau_1^{(2)}} + \frac{1}{\tau_1^{(3)}} + ... \tag{5}$$

These destruction channels can also include processes like free decays, e.g., $n \to p + e^- + \bar{\nu}_e$, which would have no dependence on the density of other particles (other than final-state blocking effects), as we previously discussed in BBN.

4.2 Relative velocity distributions

We now discuss reactions of nonrelativistic charged nuclei in a stellar plasma, where the nuclei have a distribution of velocities. The rate formula discussed above for 1+2 $\to$ 1'+2' can be generalized to take care of the velocity distribution

$$r = \frac{N_1 N_2}{1+\delta_{12}} v\sigma_{12}(v) \to \frac{N_1 N_2}{1+\delta_{12}} \langle v\sigma_{12}(v)\rangle \tag{6}$$

where $\langle\ \rangle$ represents a thermal average. Note that we have written the cross section as a function of the relative velocity v: this is ok as the total cross section is invariant under Galilean transformations (as is the rate), so it must have this form.

Now we use our Maxwell-Boltzmann velocity distribution

$$N_1 \to \int N_1(\vec{v_1}) d\vec{v_1} = N_1 \int (\frac{m_1}{2\pi kT})^{3/2} e^{-m_1 v_1^2/2kT} d\vec{v_1} \tag{7}$$

to define this thermal average

$$\langle v\sigma_{12}(v)\rangle = \int d\vec{v_1} d\vec{v_2} (\frac{m_1}{2\pi kT})^{3/2} (\frac{m_2}{2\pi kT})^{3/2} e^{-(m_1 v_1^2 + m_2 v_2^2)/2kT} \sigma_{12}(v) v \tag{8}$$

We introduce the center-of-mass and relative velocities

$$\vec{v}_{cm} = \frac{m_1\vec{v}_1 + m_2\vec{v}_2}{m_1+m_2} \qquad \vec{v}_{rel} = \vec{v} = \vec{v}_1 - \vec{v}_2 \tag{9}$$

so that

$$\vec{v}_1 = \vec{v}_{cm} + \frac{m_2\vec{v}}{m_1+m_2} \qquad \vec{v}_2 = \vec{v}_{cm} - \frac{m_1\vec{v}}{m_1+m_2} \tag{10}$$

With these definitions,

$$e^{-(m_1 v_1^2 + m_2 v_2^2)/2kT} = e^{-((m_1+m_2)v_{cm}^2 + \mu v^2)/2kT} \tag{11}$$

where $\mu = \frac{m_1 m_2}{m_1+m_2}$ is the reduced mass.

Now

$$\int d\vec{v_1} d\vec{v_2} = \int d(\frac{\vec{v_1}-\vec{v_2}}{\sqrt{2}}) d(\frac{\vec{v_1}+\vec{v_2}}{\sqrt{2}}) = \int d\vec{v} d(\frac{\vec{v_1}+\vec{v_2}}{2}) \tag{12}$$

But

$$\vec{v}_{cm} = \frac{1}{2}(\vec{v_1}+\vec{v_2}) + \frac{1}{2}(\frac{m_1-m_2}{m_1+m_2})\vec{v} \tag{13}$$

Therefore

$$\int d\vec{v}_1 d\vec{v}_2 = \int d\vec{v} \int d\vec{v}_{cm} \tag{14}$$

If we make this transformation in our expression for r, the entire dependence on $\vec{v}_{cm}$ is

$$\int d\vec{v}_{cm} e^{-(m_1+m_2)v_{cm}^2/2kT} = (\frac{2\pi kT}{m_1+m_2})^{3/2} \tag{15}$$

So we derive our desired result

$$r = \frac{N_1 N_2}{1+\delta_{12}} (\frac{\mu}{2\pi kT})^{3/2} \int d\vec{v} \sigma_{12}(v) v e^{-\mu v^2/2kT} \tag{16}$$

That is, we have the result *that the relative velocity distribution is a Maxwellian based on the reduced mass.* This can be written

$$r = \frac{N_1 N_2}{1+\delta_{12}} 4\pi (\frac{\mu}{2\pi kT})^{3/2} \int_0^\infty v^3 dv \sigma_{12}(v) e^{-\mu v^2/2kT} \tag{17}$$

In the center of mass

$$v_{cm} = 0 \Rightarrow \vec{v}_1 = \frac{-m_2}{m_1} \vec{v}_2 \tag{18}$$

so that

$$\vec{v} = \vec{v}_1 - \vec{v}_2 = \vec{v}_1 (\frac{m_1+m_2}{m_2}) \tag{19}$$

Thus

$$\vec{v}_1 = (\frac{m_2}{m_1+m_2})\vec{v} \quad \vec{v}_2 = -(\frac{m_1}{m_1+m_2})\vec{v} \tag{20}$$

leading to

$$E = E_{cm} = \frac{m_1}{2} v_1^2 + \frac{m_2}{2} v_2^2 = \frac{\mu}{2} v^2 \tag{21}$$

Therefore $dE = \mu v dv$ and

$$r = \frac{N_1 N_2}{1+\delta_{12}} \sqrt{\frac{8}{\pi\mu}} (\frac{1}{kT})^{3/2} \int_0^\infty E dE \sigma_{12}(E) e^{-E/kT}. \tag{22}$$

4.3 Nonresonant reactions

Nuclear reactions of various types can occur in stars. The first division is between charged reactions and neutron-induced reactions. The physics distinctions are the Coulomb barrier suppression of the former, and the need for a neutron source in the latter.

The charged particle reactions can also be divided in several classes. First, it is helpful to develop a general physical picture of the process 1 + 2 → 1' + 2' as the merging of 1 and 2 to form a compound nucleus, followed by the decay of that nucleus into 1' + 2'. The notion of the compound nucleus is important: a nucleus is formed that is clear unstable, as it was formed from 1+2 and therefore can decay at least into the 1+2 channel. Yet it is a long-lived state in the sense that it exists for a time much much longer than the transit time of a

nucleon to cross the nucleus. Although the picture is not entirely accurate, it is nevertheless helpful to envision the following analogy. Imagine a shallow ashtray, the bottom of which has a fairly uniform covering of marbles. Now put a marble on the flat lip of the ashtray and give it a push, so that it rolls to the bottom of the ashtray with some kinetic energy. All collisions will be assumed elastic. Thus the system that one has created is unstable: there is enough energy for the system to eject the marble back to the lip of the ashtray and thus off to infinity. But once the marble collides with the other marbles in the bottom of the ashtray, the energy is shared among the marbles. It becomes extremely improbable for one marble to get all of the energy, enabling it to escape. This is thus the picture of a compound nucleus, an unstable state that nevertheless is long lived, as it can only fission by a very improbable circumstance where one nucleon (or group of nucleons) acquires sufficient energy to escape.

If one probes a nucleus above its particle breakup threshold - this would be the intermediate nucleus in the discussion above - one will observe resonances, states that are not eigenstates but instead are unstable and thus have some finite spread in energy. You may be familiar with some examples from quantum mechanics: the case often first studied is the shape resonances that occur when scattering particles off a well, such as a square well. Such states usually carry a large fraction of the scattering strength and can be thought of as quasistationary states.

The charged particles break up into two classes, resonant (where the incident energy corresponds to a resonance) and nonresonant. The first applications we will make involve nonresonant reactions, so this is the example we will do in some detail.

A picture of a nonresonant charged particle reaction is shown in Figure 3. It depicts barrier penetration: the incident energy is well below the Coulomb barrier, so the classical turning point is well outside the region of the strong potential where fusion can occur. But this energy is not coincident with any of the resonant quasistates.

Suppose we were interested in the reaction

$$^3\mathrm{He} + {}^4\mathrm{He} \rightarrow {}^7\mathrm{Be}^* \rightarrow {}^7\mathrm{Be}(g.s.) + \gamma \tag{23}$$

where $^7\mathrm{B}e^*$ is the intermediate nucleus formed in the fusion. To calculate the cross section, it will prove sufficient to ask the following question: given the nucleus $^7\mathrm{Be}^*$, what is the probability for it to decay into the channels $^3\mathrm{He} + {}^4\mathrm{He}$ and $^7\mathrm{Be}(g.s.) + \gamma$? The former will be related by time reversal to the probability for forming the compound nucleus.

For definiteness we ask for the rate for decaying into $^3\mathrm{He} + {}^4\mathrm{He}$. This is

$$\lambda(^7\mathrm{Be}^*) = \frac{1}{\tau} = \text{prob./sec for flux of } {}^3\mathrm{He}/{}^4\mathrm{He} \text{ through a sphere at very large r}$$

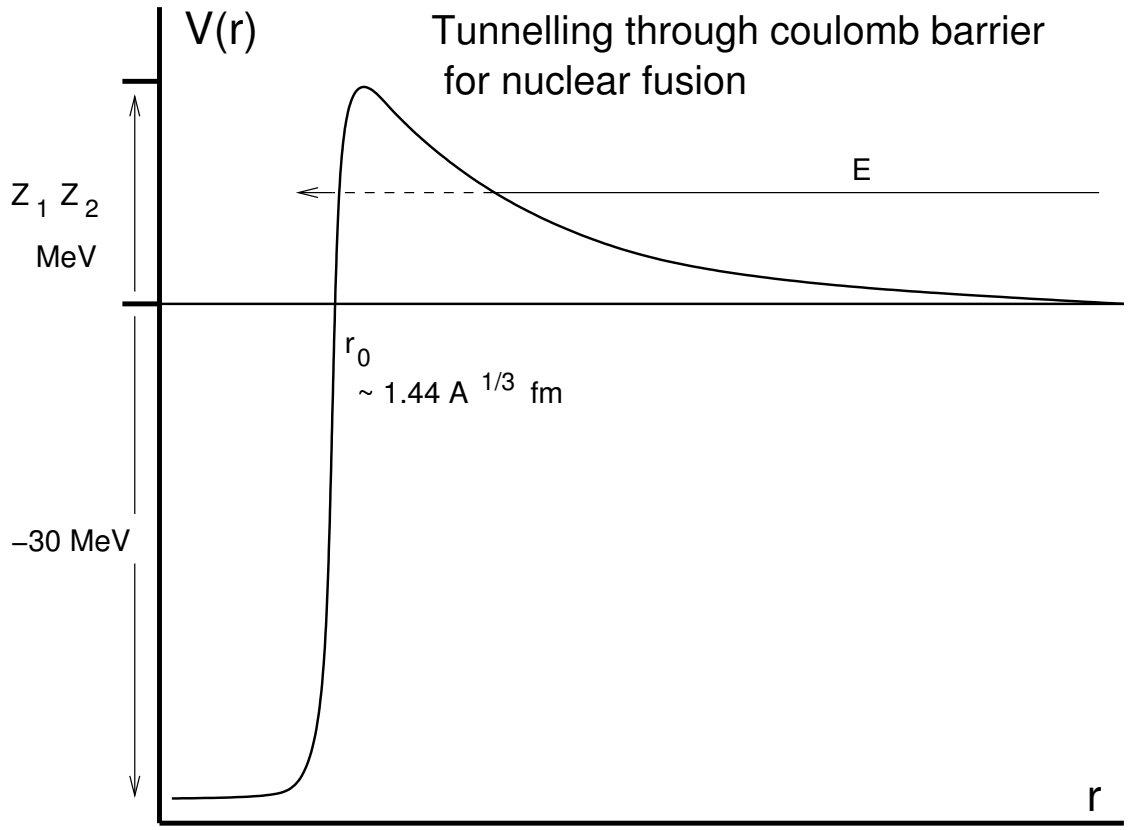

Figure 1: Sketch of the potential as a function of the distance r between two fusing nuclei. The strong force dominates for r less than r_0, roughly the nuclear radius $\sim 1.44\ \mathrm{A}^{1/3}$, with A the mass number. If the center-of-mass energy is below the Coulomb barrier, the reaction must proceed by tunneling, and is exponentially suppressed.

where r is the relative coordinate of the ^{3}He and ^{4}He. This can be written

$$v\int r^2\sin\theta d\theta d\phi|\Psi(r,\theta,\phi)|^2\Big|_{r\to\infty} = v\int|\frac{\chi_l(r)}{r}|^2|Y_{lm}|^2r^2\sin\theta d\theta d\phi\Big|_{r\to\infty} = v|\chi_l(\infty)|^2 \quad (24)$$

Note that $|\chi_l(\infty)|^2$ is a constant for very large r. We can write this result as follows

$$\lambda(^7\mathrm{Be}^*) = vP_l|\chi_l(R_N)|^2 \quad \text{where} \quad P_l = \frac{|\chi_l(\infty)|^2}{|\chi_l(R_N)|^2} \quad (25)$$

where $|\chi_l(R_N)|^2$ is a strong interaction quantity that depends on the wave function at the nuclear radius.

The penetration factor P_l, the square of the ratio of the wave function at the nuclear surface to that an infinity, will be small if the Coulomb barrier is high, as the tunneling probability would be low. A simple estimate of this can be made by assuming the attractive nuclear potential turns on sharply at radius R_N, so that outside of the matching radius one has a pure Coulomb wave function. The Coulomb radial equation is

$$(-\frac{1}{2\mu}\frac{d^2}{dr^2} + \frac{l(l+1)}{2\mu r^2} + \frac{\alpha Z_1Z_2}{r} - E)\chi_l(r) = 0 \quad (26)$$

where r is the relative ^{3}He-^{4}He coordinate. Defining

$$E = p^2/2\mu \quad \rho = pr \quad \eta = \frac{\alpha Z_1Z_2}{v} = \frac{\alpha Z_1Z_2\mu}{p} = \alpha Z_1Z_2\sqrt{\frac{\mu}{2E}}$$

and Coulomb equation can be written in its standard form

$$\frac{d^2\chi_l}{d\rho^2} + (1 - \frac{l(l+1)}{\rho^2} - \frac{2\eta}{\rho})\chi_l = 0. \quad (27)$$

The outgoing solution corresponds to the following combination of the standard Coulomb functions

$$A(G_l(\eta,\rho) + iF_l(\eta,\rho)) \underset{\text{as r}\to\infty}{\longrightarrow} A(e^{i(pr-l\pi/2-\eta\ln 2p+\sigma_l)} \sim Ae^{ipr} \quad (28)$$

Thus we find the penetration factor

$$P_l = \frac{|\chi_l(\infty)|^2}{|\chi_l(R_N)|^2} = \frac{1}{|F_l(\eta,\rho|^2 + |G_l(\eta,\rho)|^2}\Big|_{\rho=pR_N} \quad (29)$$

While the above is the exact solution in the region outside the nuclear potential, there is an approximate approach that brings out the physics more readily, illustrating both the basic penetration probability and the effects of higher partial waves and the finite nuclear radius.

The calculation, which can be found in Clayton, uses the WKB approximation, in which the Schroedinger equation is solved via an expansion in powers of $\hbar$. Thus this is a semiclassical approximation. The derivation is a bit tedious so it will not be repeated here. It yields the alternative approximate expression

$$P_l^{WKB} \sim \sqrt{\frac{2\eta}{\rho}} e^{\left[-2\pi\eta+4\sqrt{2\eta\rho}-\frac{2l(l+1)}{\sqrt{2\eta\rho}}\right]} = \sqrt{\frac{E_c}{E}} e^{\left[-\frac{2\pi\alpha Z_1 Z_2}{v}+4\sqrt{2\mu R_N^2 E_c}-\frac{2l(l+1)}{\sqrt{2\mu R_N^2 E_c}}\right]} \tag{30}$$

where $E_c = Z_1 Z_2 \alpha / R_N$ is the Coulomb potential at the nuclear surface and R_N is the nuclear radius. This expression for the penetration factor consists of three terms
• The leading Gamow factor, which also comes from the l=0 Coulomb expression we derived earlier
• The effects of the angular momentum barrier, proportional to $l(l+1)$, which suppresses the contributions of higher partial waves
• The third term shows that the nuclear radius effects the penetration: if everything else is held fixed, the larger the radius, the greater the penetration.

If we take some reaction like $^{12}\mathrm{C}(p,\gamma)^{13}\mathrm{N}$, the theory of compound nucleus reactions gives the cross section for $\alpha \to \beta$ (e.g., α = 1+2 and β = 1'+2') as

$$\sigma_{\beta\alpha} = \frac{\pi}{k^2} \frac{\Gamma_\beta \Gamma_\alpha}{(E-E_r)^2 + (\frac{\Gamma}{2})^2} \tag{31}$$

Here E_r is the energy of the nearest resonance, $\Gamma = \Gamma_\alpha + \Gamma_\beta + ...$ is the total width, and k is the wave number. Widths are related to the decay rate we have calculated by $\Gamma = \hbar\lambda$ and thus have the units of energy: the larger the width, the faster the decay, in accordance with the uncertainty principle. And $\hbar k = p$, so the wave number k has the dimensions of 1/length. Thus it is clear that the cross section so defined has the proper units. Now the definition of a nonresonant reaction is that $(E - E_r)$ is much larger that Γ, so that one is a long way from the resonance. The denominator above is then relatively smooth: it can be quite smooth if there are a number of contributing distant resonances. Noting

$$\frac{1}{k^2} \propto \frac{1}{E} \qquad \Gamma_\alpha \propto v P_l |\chi_l(R_N)|^2 \propto \sqrt{E} \frac{1}{\sqrt{E}} e^{-\frac{2\pi\alpha Z_1 Z_2}{v}} \tag{32}$$

it follows that

$$\sigma \propto \frac{1}{E} e^{-\frac{2\pi\alpha Z_1 Z_2}{v}} \tag{33}$$

motivating the definition of the S-factor

$$\sigma = \frac{1}{E} e^{-\frac{2\pi\alpha Z_1 Z_2}{v}} S(E) \propto \frac{1}{E} e^{-\frac{b}{\sqrt{E}}} S(E) \tag{34}$$

Effectively what one has done is to remove the most rapid dependence on energy, the dependence that would correspond to the s-wave interaction of two charged particles. What

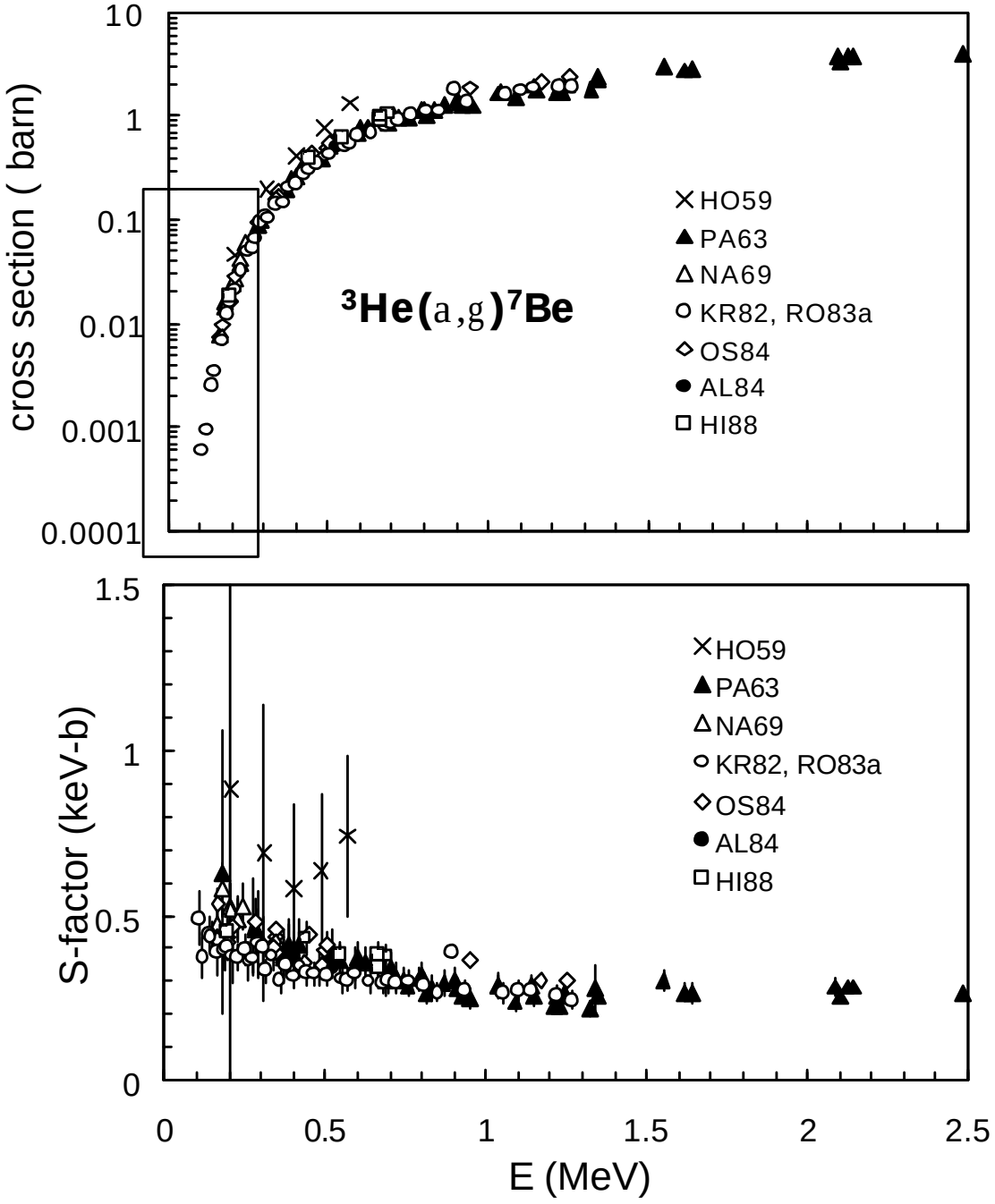

Figure 2: An illustration of the usefulness of the S-factor. The top panel shows the cross section data for ^{3}He$g(\alpha,\gamma)$, which varies by orders of magnitude as one approaches near-threshold – the energies of relevance to astrophysics. The lower panel is the corresponding S-factor – the data after s-wave point Coulomb effects are removed. The S-factor data still contains a great deal of complicated physics, including finite nuclear size effects, electron screening effects on the reaction rate, etc. But the data's much smoother behavior helps experimentalists reliably extrapolate measurements to the near-threshold region. This is important because accurate higher energy data (better statistics) can be used in a nearly linear extrapolation.

remains is a much more gently changing function S(E), which contains a lot of physics: the effects of finite nuclear size, high partial waves, etc. The importance of the S(E) is that it can be fitted to experimental cross section measurements made at energies higher than those characteristic of stars. But if S(E) evolves slowly, it can be extrapolated to lower energies that are relevant to stellar burning. This limits the need for nuclear theory: one needs to estimate the shape of S(E) as a function of E, but not its magnitude, as the magnitude can be pegged to experiment. This is the strategy followed for the nonresonant reactions of interest in solar burning.

4.4 Thermally averaged cross sections

The leading Coulomb effect - the Gamow penetration factor - is a sharply rising function of E. The Maxwell-Boltzmann distribution has an exponentially declining high-energy tail. Thus one immediately sees that $\langle \sigma v \rangle$ involves a sharp competition between these two effects, leading to some compromise most-effective-energy. This is illustrated in the figure. We can determine this energy,

$$\langle \sigma v \rangle = \sqrt{\frac{8}{\pi \mu}} (\frac{1}{kT})^{3/2} \int_0^\infty E dE e^{-E/kT} \frac{1}{E} e^{-2\pi\alpha Z_1 Z_2/v} S(E) \tag{35}$$

Recalling $v = \sqrt{2E/\mu}$ and defining $b = 2\pi\alpha Z_1 Z_2 \sqrt{\frac{\mu}{2}}$ this integral becomes

$$\sqrt{\frac{8}{\pi \mu}} (\frac{1}{kT})^{3/2} \int_0^\infty dE S(E) e^{-(E/kT + b/\sqrt{E})} \tag{36}$$

Clearly the exponential is small at small E and at large E.

Now S(E) is assumed to be a slowly varying function. The standard method for estimating such an integral, then, is to find the energy that maximizes the exponential, and expand around this peak in the integrand. This corresponds to solving

$$\frac{d}{dE}(\frac{E}{kT} + \frac{b}{\sqrt{E}}) = 0 \tag{37}$$

The solution is

$$b = \frac{2E_o^{3/2}}{kT} \tag{38}$$

We now expand the argument of the exponential around this peak energy

$$\begin{aligned} f(E) = \frac{E}{kT} + \frac{b}{\sqrt{E}} &\sim f(E_o) + (E - E_o)\frac{df}{dE_o} + \frac{1}{2}(E - E_o)^2 \frac{d^2 f}{dE_o^2} + ... \\ &= f(E_o) + f''(E_o)\frac{1}{2}(E - E_o)^2 + ... \end{aligned} \tag{39}$$

where we have used $f'(E_o) = 0$ by definition of E_o. It follows

$$\langle \sigma v \rangle \sim \sqrt{\frac{8}{\pi \mu}} (\frac{1}{kT})^{3/2} \int_0^\infty dE S(E) e^{-f(E_o)} e^{-\frac{1}{2}(E - E_o)^2 f''(E_o)}$$

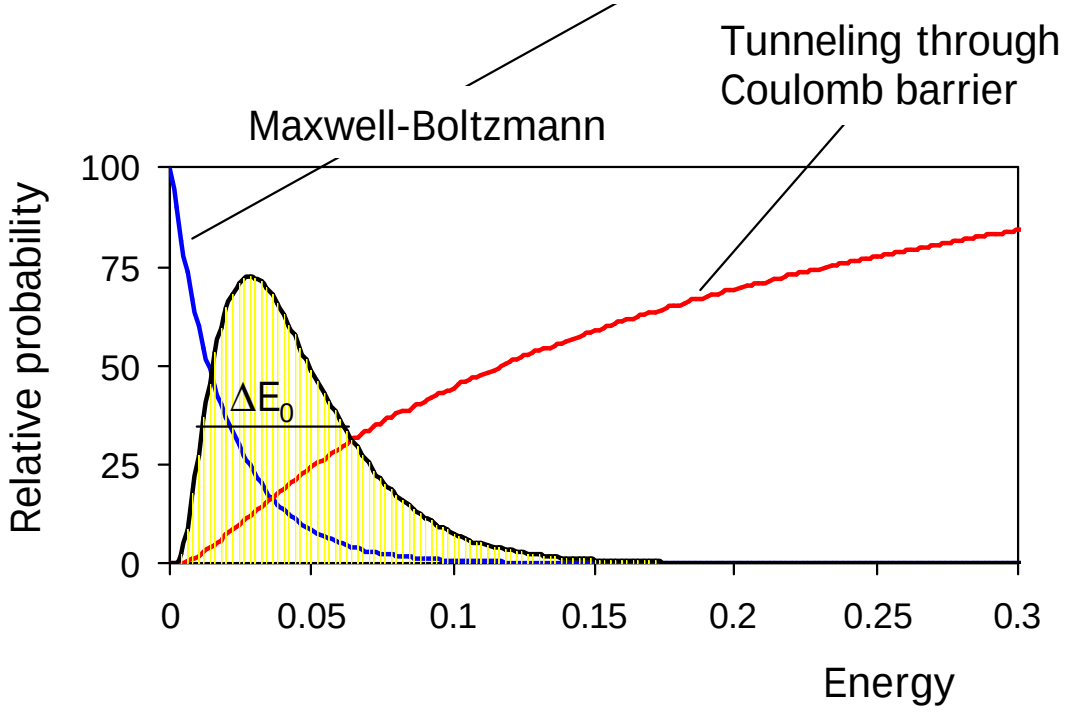

Figure 3: The relative velocity distribution in a stellar gas drops rapidly with increasing energy, while cross sections generally rise rapidly because higher energies help in overcoming the exponential suppression due to the Colomb barrier. Thus the most probably energy for a reaction involves a compromise between these two effects, and favor energies on the high-energy tail of the Boltzmann velocity distribution.

$$\sim \sqrt{\frac{8}{\pi\mu}}(\frac{1}{kT})^{3/2}S(E_o)e^{-f(E_o)}\int_{-\infty}^{\infty}dEe^{-\frac{1}{2}(E-E_o)^2f''(E_o)} \tag{40}$$

In deriving this result, we have assume S(E) is slowly varying in the vicinity of the integrand peak at E_o, and thus can be replaced by its value at the peak. Note our formula could easily be improved by doing a Taylor expansion on S(E), e.g.,

$$S(E) \sim S(E_o) + (E - E_o)\frac{dS}{dE_o} + ... \tag{41}$$

Thus our final answer would have an additional contribution due to $S'(E_o)$.

But if we just keep $S(E_o)$, the integral can be done, yielding

$$\int_{-\infty}^{\infty}dEe^{-\frac{1}{2}(E-E_o)^2f''(E_o)} = \sqrt{\frac{2\pi}{f''(E_o)}} \tag{42}$$

so that

$$\langle\sigma v\rangle = \frac{4}{\sqrt{\mu}}(\frac{1}{kT})^{3/2}S(E_o)\frac{e^{-f(E_o)}}{\sqrt{f''(E_o)}} \tag{43}$$

Now

$$f''(E_o) = \frac{3b}{4E_o^{5/2}} = \frac{3}{2E_okT} \qquad f(E_o) = \frac{E_o}{kT} + \frac{b}{\sqrt{E_o}} = \frac{3E_o}{kT} \tag{44}$$

Thus

$$\begin{aligned}\langle\sigma v\rangle &= \frac{4}{\sqrt{\mu}}(\frac{1}{kT})^{3/2}S(E_o)e^{-3E_o/kT}\sqrt{\frac{2E_okT}{3}} \\ &= \frac{16}{9\sqrt{3}}\frac{1}{\mu}\frac{1}{2\pi\alpha Z_1Z_2}S(E_o)e^{-3E_o/kT}(\frac{3E_o}{kT})^2.\end{aligned} \tag{45}$$

Now we define a quantity A by

$$AM_N = \frac{A_1A_2}{A_1 + A_2}M_N \sim \frac{m_1m_2}{m_1 + m_2} = \mu \tag{46}$$

where M_N is the nucleon mass. Substituting this in, evaluating some constants, and dividing out the dimensions of S (note S has the units of a cross section times energy) yields

$$r_{12} \equiv \frac{N_1N_2}{1 + \delta_{12}}\langle v\sigma_{12}(v)\rangle = \frac{N_1N_2}{1 + \delta_{12}}(7.21{\cdot}10^{-19}\mathrm{cm}^3/\mathrm{sec})\frac{1}{AZ_1Z_2}\frac{S(E_o)}{\mathrm{keV\ barns}}e^{-3E_o/kT}(\frac{3E_o}{kT})^2 \tag{47}$$

Note that the overall dimensions are clearly $1/(\mathrm{cm}^3\mathrm{sec})$, as the number densities have units $1/\mathrm{cm}^3$. Also remember that a barn = 10^{-24} cm^2.

Now E_o defines the peak of the contributions to $\langle v\sigma \rangle$. From its definition

$$E_o = (\frac{ktb}{2})^{2/3} \quad \Rightarrow \quad \frac{E_o}{kT} = (\frac{\pi\alpha Z_1 Z_2}{\sqrt{2}})^{2/3}(\frac{\mu c^2}{kT})^{1/3} \tag{48}$$

where the speed of light has been reinserted to make it explicit that this quantity carries no units. For example, in the center of our sun $kT \sim 1.5 \cdot 10^7$K ~ 1.3 keV. So if we plug in the appropriate numbers for the ^{3}He+^{3}He reaction one finds

$$E_o \sim 16.5kT \sim 21.5\text{keV} \tag{49}$$

One could compare this to the average energy of a Maxwell- Boltzmann distribition of paticles of $\langle$ E $\rangle \sim 3$ kT. Thus, indeed, the reactions are occurring far out on the Boltzmann tail, where nuclei have a better chance of penetrating the Coulomb barrier.

It might be helpful at this point to walk through the example of ^{12}C+p going to ^{13}N. If we define the zero of energy as that of the ^{12}C nucleus and proton at rest, then ^{13}N is bound by 1.943 MeV. Furthermore there is a resonance in ^{13}N at 2.367 MeV, 424 keV above the zero of energy. Thus a ^{12}C+p collision at a center-of-mass energy of 424 keV would be directly on resonance. In the lab frame, this corresponds to a 460 keV proton incident on a ^{12}C nucleus at rest.

The cross section is

$$\sigma = \frac{1}{E}S(E)e^{\frac{-2\pi\alpha Z_1 Z_2}{v}} = \frac{\pi}{k^2}\frac{\Gamma_p(E)\Gamma_\gamma}{(E-E_r)^2 + (\Gamma/2)^2} \tag{50}$$

One can reexpress the S-factor, then, as

$$S(E) = \frac{\pi}{2\mu}\frac{\Gamma_\gamma}{(E-E_r)^2 + (\Gamma/2)^2}\left(e^{2\pi\alpha Z_1 Z_2/v}\Gamma_p(E)\right) \tag{51}$$

Now the product of the exponential and Γ_p on the right should be roughly energy independent, as the exponential cancels the penetration probability buried in Γ_p. Thus the assumption the S(E) is weakly energy dependent requires that one not be too close to the resonance.

If one examines this system experimentally, the results are as shown in the Figures 6. Note that S(E) is quite smooth for E $\lesssim$ 300 keV. Thus data in the 100-300 keV range can be used to extrapolate the measured cross section to the region of interest for p burning via the CNO cycles. In contrast, the raw cross section varies over 9 orders of magnitude. Note that the theory curve, which takes into account the resonance, does quite well throughout the illustrated region. Thus the success of theory in the 100-400 keV region gives one great confidence that the values extrapolated to 20-50 keV are correct. The sharp steeping of $S(E)$ above 400 keV lab energy is a clear indication of the resonance at 460 keV lab proton energy.

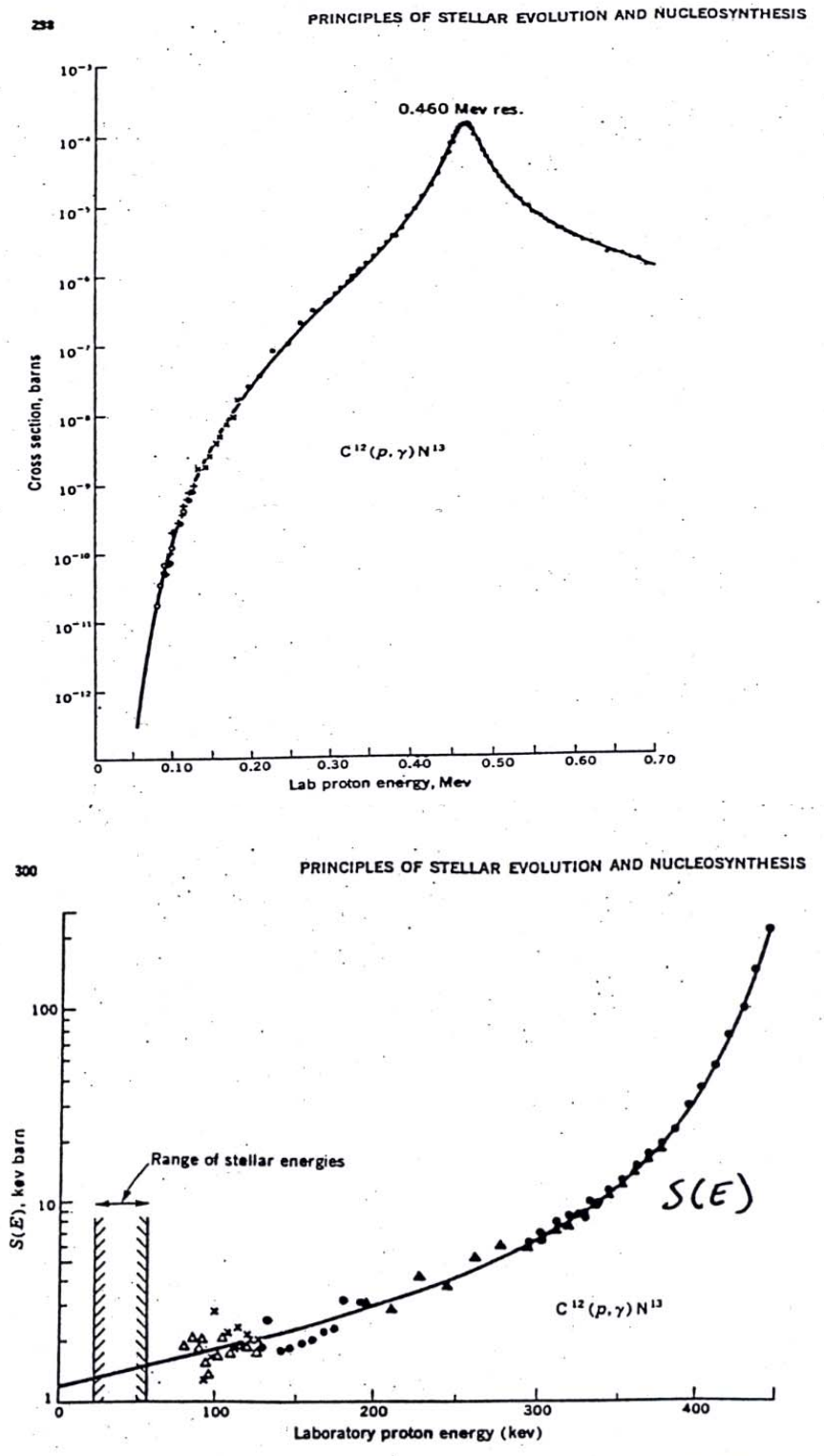

Figure 4: The data for ^{12}C(p,γ) and the resulting S-factor. The energies of astrophysical interest are around 30 keV, where the cross section data are very steeply falling due to Colomb effects.

What about resonant reactions? That is, suppose we had some astrophysical setting where the relevant value of E_o was not as above ($\sim$ 35 keV), but in fact sat on the resonance at 424 keV center-of-mass energy? If the resonance is narrow (usually the case) compared to the typical spred of relevant energies of the colliding nuclei,

$$\begin{aligned}\langle \sigma v \rangle &= \sqrt{\frac{8}{\pi\mu}}(\frac{1}{kT})^{3/2}\int_0^\infty EdEe^{-E/kT}\frac{\pi}{2\mu E}\frac{\Gamma_p\Gamma_\gamma}{(E-E_r)^2+(\Gamma/2)^2} \\ &\sim \sqrt{\frac{8}{\pi}}\frac{\pi}{2}(\frac{1}{\mu kT})^{3/2}\Gamma_p\Gamma_\gamma e^{-E_r/kT}\int_{-\infty}^\infty dE\frac{1}{(E-E_r)^2+(\Gamma/2)^2} \end{aligned} \quad (52)$$

The integral is $2\pi/\Gamma$, so

$$\langle \sigma v \rangle_{\rm resonant} = (\frac{2\pi}{\mu kT})^{3/2}\frac{\Gamma_p\Gamma_\gamma}{\Gamma}e^{-E_r/kT} \quad (53)$$

If the only open channels for decay of the compound nucleus are proton and γ emission, then $\Gamma = \Gamma_p + \Gamma_\gamma$. If Γ_p greatly exceeds Γ_γ, then $\frac{\Gamma_p\Gamma_\gamma}{\Gamma} \sim \Gamma_\gamma$. That is, the rate depends only on the γ width. The opposite limit, a very small Γ_p, which might occur in a low energy resonance in a high Z target, yields a rate that depends only on Γ_p, which governs the formation probability of the compound nucleus.

Equation (47) shows how the rate can be expressed in terms of the S-factor. This equation – and various embellishments that account for variations in $S(E)$ – is the usual way experiments convert their lab cross section measurements into a form that is more readily used by astrophysicists. In fact, several standard references provide both numerical values and attractive fitting formulas for $\langle v\sigma \rangle$, that then can be used in BBN or stellar structure calculations. Standard sources for Maxwellian-averaged cross sections include

- neutron-induced reactions: The National Nuclear Data Center's Evaluated Nuclear Data File (ENDF) astrophysics database, http://www.ndc.bnl.gov/astro/
- charged particles: NACRE compilation, http://pntpm3.ulb.ac.be/Nacre/barre_database.htm
- charged particles: Caughlin and Fowler, Atomic Data and Nuclear Data Tables 40 (1988) 283 for cross sections not given in NACRE

4.5 The standard solar model and the Lane-Emden Polytrope Solution

We now start a discussion of stars that burn hydrogen through the pp and CNO cycles, such as our sun and similar stars. Almost all stars lying along the main sequence - perhaps 80% of the stars we observed - are thought to be hydrogen burning. The main sequence is a track of stars in the Hertzsprung-Russell diagram, or HR diagram. The HR diagram is a plot of stars on a plane where the vertical axis is the luminosity and the horizontal axis is the surface temperature (as measured by the color of the star). Stellar luminosities vary from $(10^{-4} - 10^6)$ that of our sun, with surface temperatures vary from 2000-50000K.

The most obvious properties that one can use to characterize a star are its surface temperature T_s, luminosity L, and radius R. The former two are accessible to observation, but generally the radius is not. Yet it is easy to see that there is a relationship between these properties. If we pretend stars radiate as black bodies, then the energy emitted per unit time per unit surface area is given by the Stefan-Boltzmann black-body radiation law, σT_s^4, where $\sigma = 5.67 \times 10^{-5}\text{ergs/K}^4\text{/s/cm}^2$. Thus the star's luminosity is

$$L = 4\pi R^2 \sigma T_s^4 \tag{54}$$

We can normalize things to solar properties to rewrite this as

$$\frac{L}{L_{solar}} = (\frac{R}{R_{solar}})^2 (\frac{T_s}{T_{solar}})^4. \tag{55}$$

Though this result is true only for a blackbody, it makes it plausible that a plot of luminosity vs. temperature might yield a one-dimensional path in the plane parameterized by the radius, and thus the mass, of the star, provided that the stars have similar internal structure. For example, if a class of stars radiated as blackbodies, the trajectory would be as described above.

This was basically the discovery of Hertzsprung and Russell. The HR diagram on the next page shows a dominant trajectory - the main sequence - running from high temperature to low temperature. It also shows other classes of stars that reside well off the main sequence. The sun is situated on the main sequence according to its observed surface temperature of about 6500 K. Stars at the upper left - on the main sequence with temperatures 4 times that of the sun and luminosities 6 orders of magnitude larger - would have a radius about 60 times that of our sun. The red, cool, dwarf stars in the lower right of the main sequence, with luminosities about 2000 times lower than the sun and temperatures about half that of the sun, have radii about 0.1 that of the sun. Other classes of stars are well separated from the main sequence. One group has luminosities on the order of 10^4 and temperatures again about half that of the sun. Thus these supergiants would correspond to a radius about 400 times that of the sun. Red giants, which form another patch off the main sequence, have a radius about 50 times that of our sun. White dwarfs - with luminosities about 1/200 of solar and temperatures twice solar - would correspond to a radius of about 1/50th that of the sun. These sit well below the main sequence.

The sun is our "test case" for developing a theory of main-sequence stellar evolution. We know far more about this star - its age, luminosity, radius, surface composition, and even its neutrino luminosity and helioseismology - that any other star. Solar models trace the evolution of the sun over the past 4.6 billion years of main sequence burning, thereby predicting the present-day temperature and composition profiles of the solar core that govern energy production. Standard solar models share four basic assumptions:

• The sun evolves in hydrostatic equilibrium, maintaining a local balance between the gravitational force and the pressure gradient. To describe this condition in detail, one must

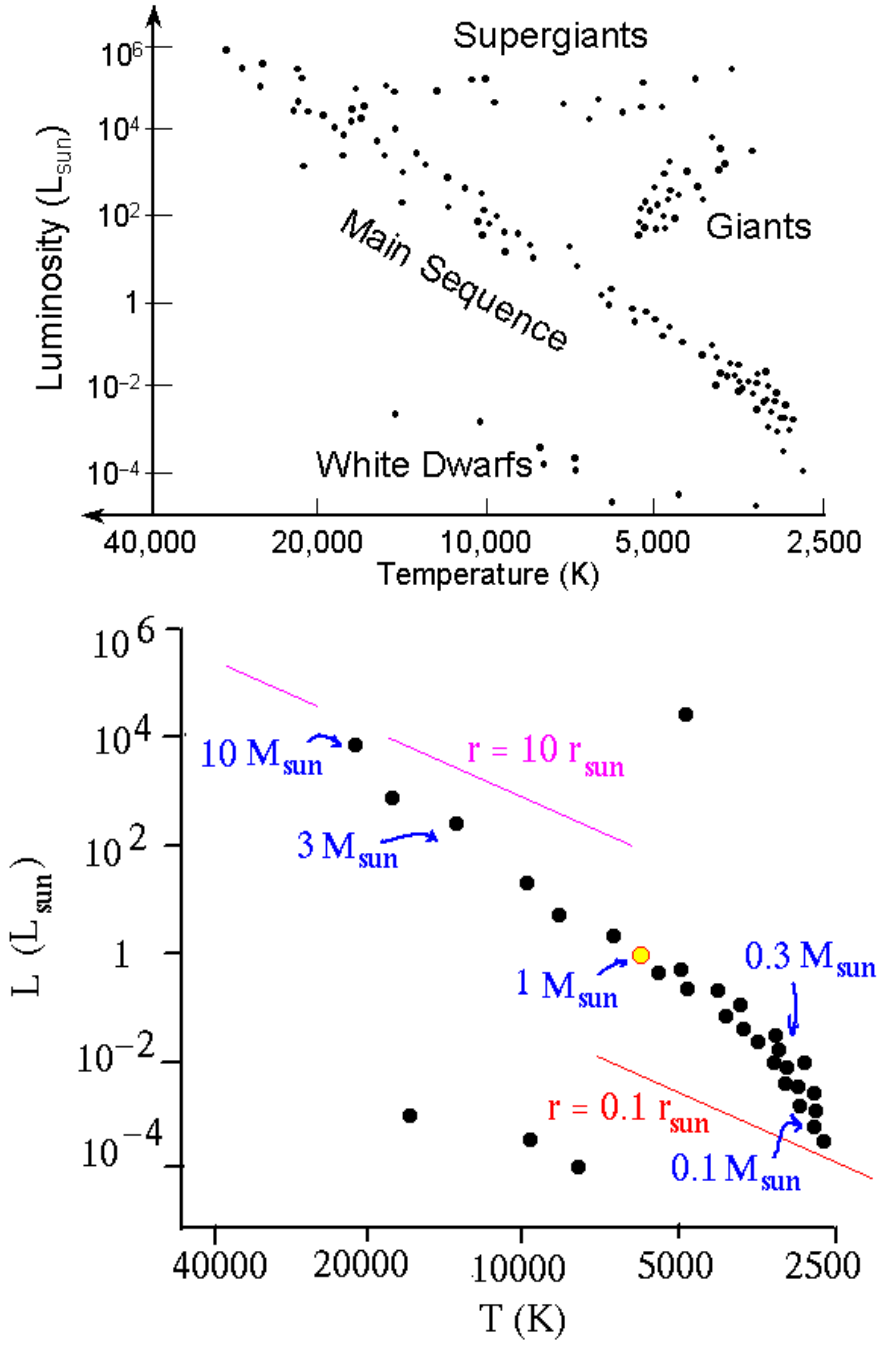

Figure 5: Two schematic diagrams showing main-sequence sections of the HR diagram, including the position of our sun.

specify the equation of state as a function of temperature, density, and composition.

• Energy is transported by radiation and convection. While the solar envelope is convective, radiative transport dominates in the core region where thermonuclear reactions take place. The opacity depends sensitively on the solar composition, particularly the abundances of heavier elements.

• Thermonuclear reaction chains generate solar energy. The standard model predicts this energy is produced from the conversion of four protons into ^{4}He.

$$4p \rightarrow^4 \mathrm{He} + 2e^+ + 2\nu_e$$

About 98% of the time this occurs through the pp chain, with the CNO cycle contributing the remaining 2%. The sun is a large but slow reactor: the core temperature, $T_c \sim 1.5 \cdot 10^7$ K, results in typical center-of-mass energies for reacting particles of $\sim$ 10 keV, much less than the Coulomb barriers inhibiting charged particle nuclear reactions. Thus reaction cross sections are small, and one must go to significantly higher energies before laboratory measurements are feasible. These laboratory data must then be extrapolated to the solar energies of interest, as we discussed previously.

• The model is constrained to produce today's solar radius, mass, and luminosity. An important assumption of the standard model is that the sun was highly convective, and therefore uniform in composition, when it first entered the main sequence. It is furthermore assumed that the surface abundances of metals (nuclei with A $>$ 5) were undisturbed by the subsequent evolution, and thus provide a record of the initial solar metallicity. The remaining parameter is the initial ^{4}He/H ratio, which is adjusted until the model reproduces the present solar luminosity after 4.6 billion years of evolution. The resulting ^{4}He/H mass fraction ratio is typically 0.27 ± 0.01, which can be compared to the big-bang value of 0.23 ± 0.01. (Note that today's surface abundance can differ from this value due to diffusion of He over the lifetime of the sun.) Note that the sun was formed from previously processed material.

The "standard solar model" is the terminology used to describe models, such as that of Bahcall and Pinsonneault, that implement the above physics in a computer code, then evolve the sun forward from the onset of main sequence burning. Generally calculations are one-dimensional, which means that the physics such as convection can not arise dynamically. It can, and sometimes is, put in phenomenologically, through approximations such as "mixing length theory."

The model that emerges is an evolving sun. As the core's chemical composition changes, the opacity and core temperature rise, producing a 44% luminosity increase since the onset of the main sequence. Some other features of the sun evolve even more rapidly. For example, the ^{8}B neutrino flux, the most temperature-dependent component, proves to be of relatively recent origin: the predicted flux increases exponentially with a doubling period of about 0.9

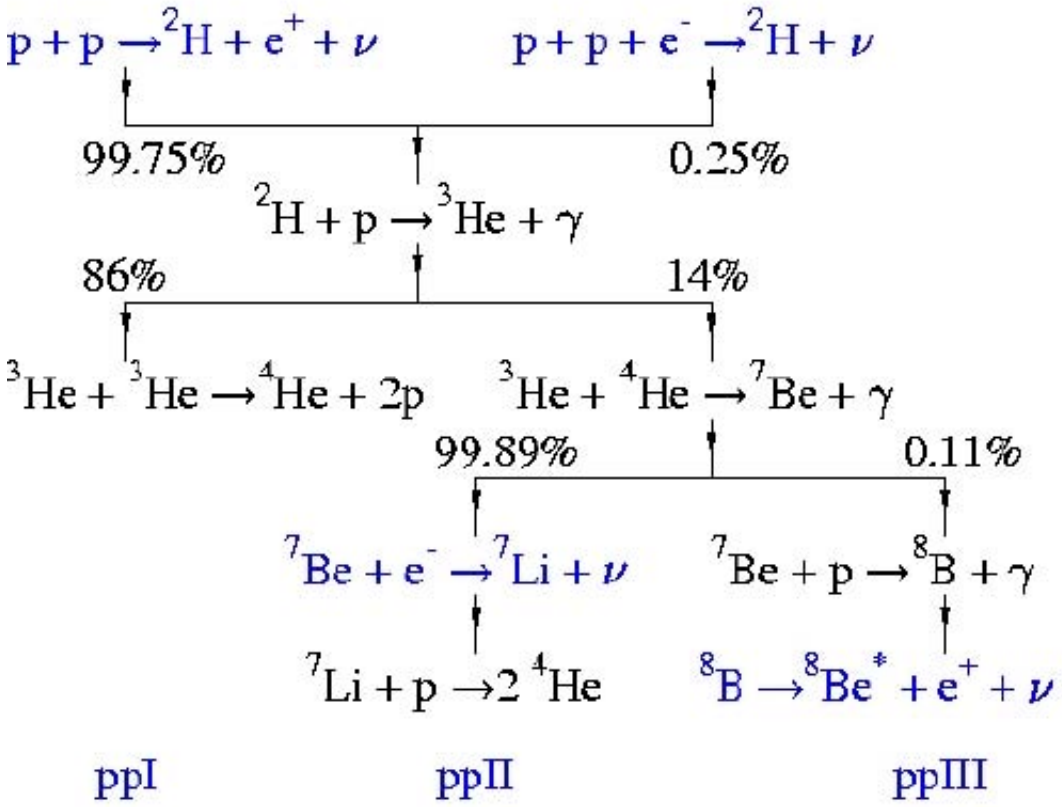

Figure 6: The pp chain, showing the terminations corresponding to the competing ppI, ppII, and ppIII cycles. Note the cycles are "tagged" by associated characteristic neutrinos.

billion years. This is the flux to which Ray Davis's famous Homestake gold mine experiment is primarily sensitive. As another example of a time-dependent feature of the sun, the equilibrium abundance and equilibration time for ^{3}He are both sharply increasing functions of the distance from the solar center. Thus a steep ^{3}He density gradient is established over time. We will shortly see that the ^{3}He is sort of a "caltalyst" in the pp chain, being produced and then consumed as an intermediate step in synthesizing ^{4}He.

Such models generally do not model the earliest history of our sun, when it first formed as a body of gas contracting under its own gravity, heating and ionizing as the gravitational work is done. The early contraction of the sun, when it approaches the main sequence vertically from above in the HR diagram, is characterized by high luminosity and convection throughout the star, lasting for a few million years. (Actually, there is thought to be continued convection in the core of sun for perhaps 10^8 years, though this is driven by another mechanism: the fact that the CNO cycle is burning out of equilibrium due to initials metals in the sun.) The core of the sun reaches radiative equilibrium first, and this region then grows outward.

But there are shortcomings in the standard solar model. Li had to be burned at some point in the sun's evolution to account for the fact that the solar surface abundance is roughly 1/100th that found in meteorites. Perhaps this is due to the failure to model the sun's early convective stage. Or perhaps material can be pulled below the convective envelope by some mechanism, to a depth where the higher temperature allows ^{7}Li(γ,^{3}He)^{4}He to occur.

Now a realistic standard solar model, even if restricted to 1D (as is usually the case) is a nontrivial numerical problem: the radiative transport requires detailed opacities, which depend on composition, the energy production also depends on composition and on compositions that are established as the pp-chain evolves, etc. However, much simpler (and less dynamic) toy models exist which are not too unrealistic. One set is these comes from the Lane-Emden equation, which provide a solution with a total mass and radius, for a given polytrope (defined below).

Consider a spherically symmetric star governed by the following equations

$$\begin{aligned} \frac{dp(r)}{dr} &= -\frac{Gm(r)}{r^2}\rho(r) \\ \frac{dm(r)}{dr} &= 4\pi r^2 \rho(r) \\ p(r) &= k\rho^\gamma \;\Rightarrow\; \frac{p}{p_0} = \left(\frac{\rho}{\rho_0}\right)^\gamma \end{aligned} \tag{56}$$

Here $p(r)$ and $\rho(r)$ are the star's pressure and density profile, with p_0 and ρ_0 the central pressure and density. The first equation is hydrostatic equilibrium. The second defines the contained mass as a function of ρ. And the third is a simplifying assumption that the

equation of state is defined by a single adiabatic index γ, where

$$\gamma \equiv \frac{c_p}{c_v} = 1 + \frac{1}{n} = \frac{n+1}{n} \tag{57}$$

is the ratio of the specific heats, and where n is the polytrope index. Different choices of n are appropriate for different stars. The best approximation to stars like the Sun is $n = 3$.

Introduce the function

$$\Phi(r) \equiv \left(\frac{\rho(r)}{\rho_0}\right)^{\gamma-1} = \left(\frac{p(r)}{p_0}\right)^{\frac{\gamma-1}{\gamma}} \tag{58}$$

Then

$$\frac{d\Phi(r)}{dr} = \frac{\gamma-1}{\gamma}\left(\frac{p(r)}{p_0}\right)^{\frac{-1}{\gamma}} \frac{1}{p_0}\frac{dp(r)}{dr} = \frac{\gamma-1}{\gamma}\frac{\rho_0}{\rho(r)}\frac{1}{p_0}\frac{dp(r)}{dr} = \frac{\gamma-1}{\gamma}\frac{\rho_0}{p_0}\left(\frac{-Gm(r)}{r^2}\right) \tag{59}$$

where we have used the hydrostatic equilibrium equation in the last step. Thus

$$\begin{aligned} m(r) &= -\frac{1}{G}\frac{\gamma}{\gamma-1}\frac{p_0}{\rho_0}r^2\frac{d\Phi(r)}{dr} \\ \Rightarrow \frac{dm(r)}{dr} &= -\frac{1}{G}\frac{\gamma}{\gamma-1}\frac{p_0}{\rho_0}\frac{d}{dr}\left(r^2\frac{d\Phi(r)}{dr}\right) = 4\pi r^2\rho(r) = 4\pi r^2\rho_0\Phi(r)^{\frac{1}{\gamma-1}} \\ \Rightarrow \quad & \frac{2}{r}\frac{d\Phi(r)}{dr} + \frac{d^2\Phi(r)}{dr^2} = -4\pi G\frac{\gamma-1}{\gamma}\frac{\rho_0^2}{p_0}\Phi(r)^{\frac{1}{\gamma-1}} \end{aligned} \tag{60}$$

Now define the dimensionless coordinate $x = r/r_x$ where

$$r_x = \left[\frac{p_0\gamma}{4\pi G\rho_0^2(\gamma-1)}\right]^{1/2} \tag{61}$$

and we obtain the Lane-Emden equation

$$\frac{d^2\Phi(x)}{dx^2} + \frac{2}{x}\frac{d\Phi(x)}{dx} + \Phi(x)^{\frac{1}{\gamma-1}} = 0 \tag{62}$$

This must be solved with the boundary conditions $\rho(0) = \rho_0$ and $\rho'(0) = 0$ which yield

$$\Phi(0) = 1 \quad \Phi'(0) = 0 \tag{63}$$

The $n = 3$ ($\gamma = 4/3$) polytrope provides a good description of stars like our sun. We evaluate $\Phi(x)$ with NDSolve on Mathematica. With that solution we then

- Solve for $\Phi(x) == 0$, finding x=6.89685, which we will use to determine the stellar radius below, as at this point the pressure and density vanish.
- Integrate $x^2\Phi(x)^{1/(\gamma-1)}$ from 0 to 6.89685, as we will be able to relate this quantity tio the solar mass. This integral is 2.01824.

How should pick parameters for the Sun? We will use the central density of the Sun as the control parameter, picking a value of 148 g/cm^3 for this exercise, as this is the value found in more sophisticated SSMs. We can use the fact that we know the solar mass. So

$$1.99 \times 10^{33}\mathrm{g} = \int_0^{\mathrm{R_s}} r^2 dr 4\pi\rho(r) = 4\pi r_x^3 \rho_0 \int_0^{6.8968} dx\ x^2 \Phi(x)^{1/(\gamma-1)} = 4\pi r_x^3 \rho_0 (2.01824) \quad (64)$$

From which we find $r_x = 8.0935 \times 10^9$ cm. This fixes the solar radius in our simple model

$$R_s = 6.89685 r_x = 5.582 \times 10^{10}\mathrm{cm} \quad (65)$$

which can be compared to the observed value of 6.96 $\times 10^{10}$ cm. From r_x we can then evaluate p_0,

$$p_0 = r_x^2 \frac{\gamma - 1}{\gamma} 4\pi G \rho_0^2 = 3.01 \times 10^{17}\mathrm{ergs/cm}^3 \quad (66)$$

which can be compared to the SSM central core value of 2.29 $\times 10^{17}$ ergs/cm^3. The resulting density and pressure profiles are shown in Figs. 7 and 8.

Now we can use the fact that the solar equation of state is approximately that of a perfect gas, $P(r) = n(r)kT(r)$ where n is the number density, to determine the temperature profile. (But see below for some comments.) Here $n = n_I + n_e$ is the number of ions and electrons in the plasma. Now

$$n_I = \rho N_A \sum_i \frac{X_i}{A_i} \equiv \frac{\rho N_A}{\mu_I} \quad \text{where} \quad \mu_I = \left[\sum_i \frac{X_I}{A_i} \right]^{-1} \quad (67)$$

where X_i and A_i are the mass fraction and mass number of species i, and μ_I is the molecular weight. If our gas consists of hydrogen with mass fraction X and helium, then

$$\mu_I^{-1} \sim X + \frac{(1-X)}{4} = \frac{1+3X}{4} \quad (68)$$

Similarly for the electrons

$$n_e = \rho N_A \sum_i \frac{X_i Z_i f_i}{A_i} \sim \rho N_A \sum_i \frac{X_i Z_i}{A_i} \equiv \frac{\rho N_A}{\mu_e} \quad \text{where} \quad \mu_e = \left[\sum_i \frac{X_i Z_i}{A_i} \right]^{-1} \quad (69)$$

where we have made the approximation above that the ionization fraction f_i=1, which is a good approximation in the hot energy-producing solar core. Now if everything except hydrogen has $Z = N$ then

$$\mu_e^{-1} = X + \frac{(1-X)Z}{2Z} = \frac{1+X}{2} \quad (70)$$

so that

$$n = n_i + n_e = \rho N_A \left[\frac{1}{\mu_I} + \frac{1}{\mu_e} \right] \equiv \frac{\rho N_A}{\mu} \quad \text{where} \quad \frac{1}{\mu} \sim \frac{3+5X}{4} \quad (71)$$

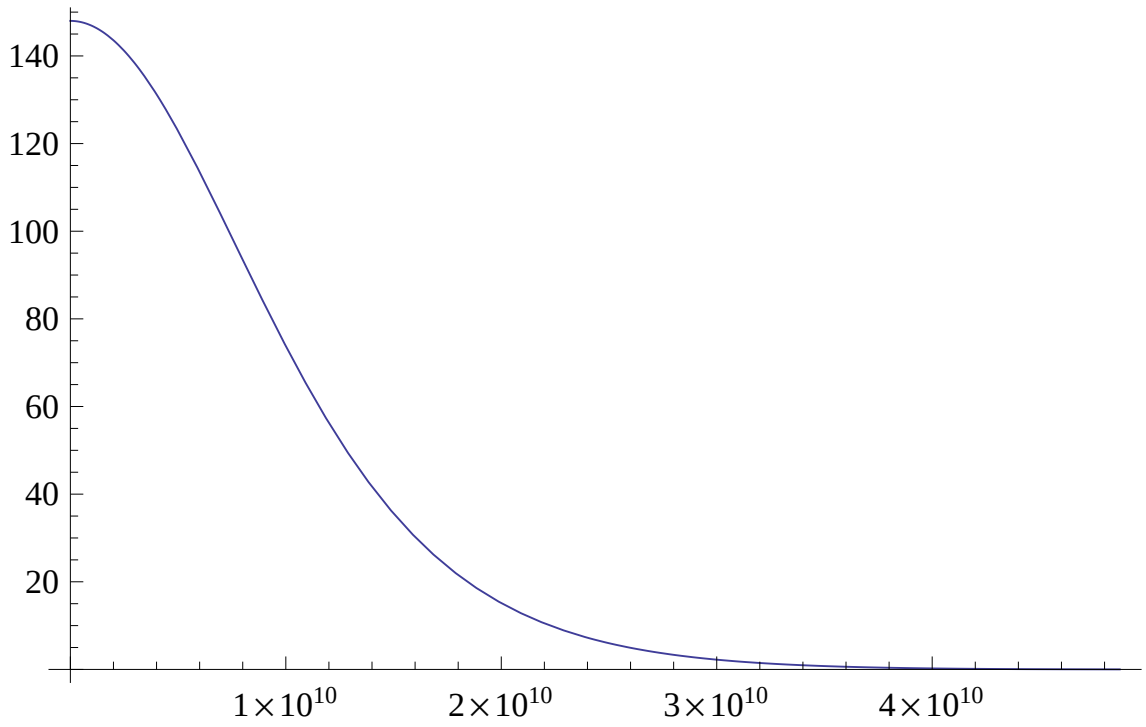

Figure 7: The Lane-Emden n=3 polytrope solution for the solar density profile (units of g/cm^3) as a function of radius (in cm). The solar surface is at r=5.582 $\times 10^{10}$ cm.

under the approximations described above. Consequently

$$P = \rho N_A \left[\frac{3+5X}{4}\right] kT \tag{72}$$

where it is implicit the P, ρ, and X are also functions of r. If one knows $X(r)$, one can calculate $T(r)$ in the Lane-Emden model described above. In the SSM at $r = 0$ $X \sim 0.341$, from which one then finds $T_c \sim 1.48 \times 10^7$K. This compares to the SSM value of 1.56×10^7K. By looking up $X(r)$ from the SSM, we could calculate the temperature at other rs too.

In fact, we can do much better than this. One can convert this simple - but realistic, as seen above - model into an evolutionary model. At time $t = 0$, the beginning of the main sequence, the standard assumption (as we have noted) is a homogeneous Sun. X would then be independent of r, a great simplification. Its value would be around 0.72, slightly smaller than the primordial value since our Sun was created 9 b.y. after the Big Bang, and thus was formed from material that had been processed by earlier generations of stars. We could then pick a value for ρ_0 to start things off. As $X(r)$ is initially independent of r, we would know the temperature everywhere. Now we evolve for a time step Δt. By putting in the nuclear reactions for the pp chain, at $t = 0 + \Delta t$ we could evaluate the produced ^{4}He (as well as the amount of ^{3}He) as a function of r. All of the production would be near the star's center. We would then have $\mu(r)$ at that time, and thus we could evaluate $T(r)$. Then we

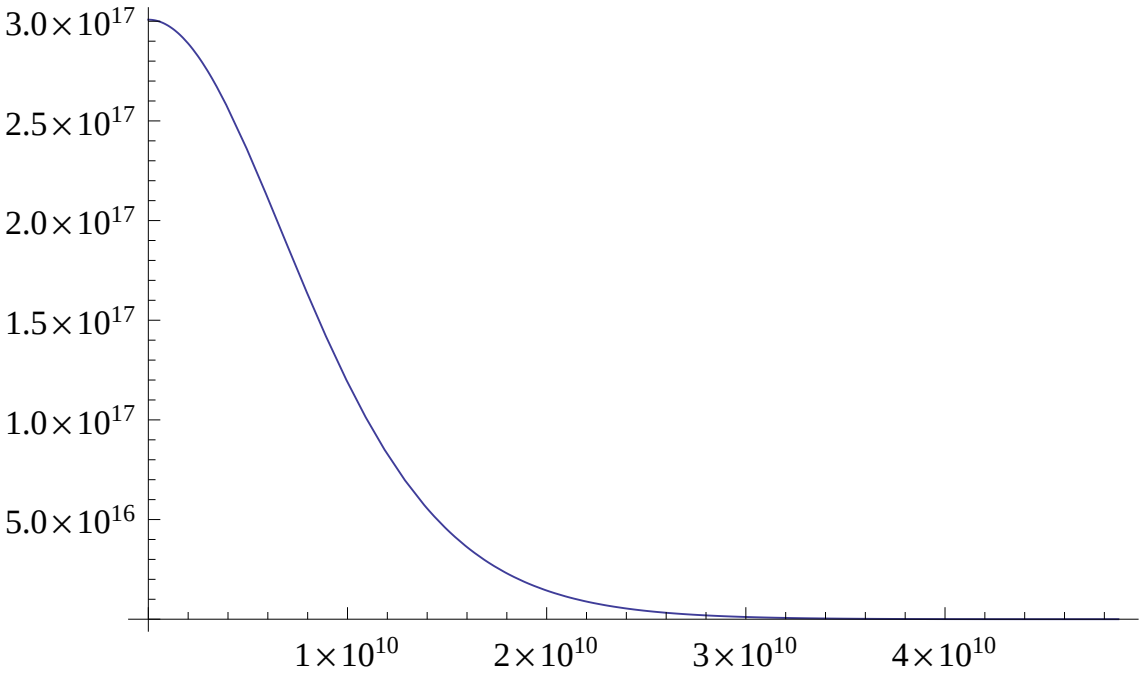

Figure 8: As in Fig. 7, but for the solar pressure profile (units of erg/cm^3).

take another step. We continue until today, $t = 4.55$ b.y., a time we know from various solar system chronometers. At $t = 4.55$ b.y. we could then evaluate the luminosity: this would be the total energy produce in the $4p \rightarrow {}^4$He reaction, minus a correction due to omitted neutrinos. But the solar constant is known. So if we fail to reproduce the correct result, we go back to square one, and pick a new ρ_0 and repeat. When this converges, we have a model with the correct mass, age, and luminosity. ρ_0 is no longer an input parameter, but a prediction. The only input is $X(r) = constant$ at time $t = 0$, a quantity that we think is reasonably well known.

The model that emerges is nontrivial. We can predict the H and He density gradients. We could study the evolution of the luminosity with time (which should give us a surprising result). We can study the evolution of neutrino fluxes with time. We can predict interesting gradients that evolve over solar times, like the ^{3}He gradient (see next section). All of the physics will follow if we can just put in the needed nuclear physics. In fact, our basic equations already qualitative show very interesting physics. For example, Eq. (72) shows that as X drops (as ^{4}He is created), T will need to increase to provide the pressure needed to stabilize the star. That is, the Sun gets hotter as it evolves.

Why is the Sun an $n = 3$ polytrope? While the Sun's EOS is dominated by gas pressure (we assumed this above), there is also a contribution from radiation. Thus the total pressure is

$$P = P_{\rm gas} + P_{\rm radiation} = \frac{\rho N_A}{\mu} kT + \frac{1}{3} a (kT)^4 \tag{73}$$

where the gas constant $a = \pi^2/15$, from Chapter 3. Now assume $\beta = P_{\rm gas}/P$ is constant. Then

$$P = \frac{1}{\beta}\frac{\rho N_A}{\mu}kT \quad \text{and} \quad 1-\beta = \frac{P_{\rm radiation}}{P} = \frac{1}{3}a(kT)^4\frac{1}{P} \tag{74}$$

Eliminating T between these two equations yields

$$P = \left(\frac{1-\beta}{\beta^4}\right)^{1/3}\left(\frac{3N_A^4}{a\mu^4}\right)^{1/3}\rho^{4/3} \tag{75}$$

Thus $\gamma = 4/3$ and n=3. The observation that main sequence stars have roughly constant β is thus the reason for taking n=3. For the Sun, $\beta \sim 0.9993$.

4.6 The pp-chain

Now let's turn to the pp chain. The controlling reaction of the chain is the initial reaction, the β decay of two protons in a plasma. This weak interaction is the mechanism by which the Sun produces neutrons, the necessary step in creating He. The slowness of this reaction accounts for the long expected lifetime of the Sun, about 10 b.y.

The p+p cross section is

$$\sigma = \int \frac{1}{|\vec{v}_1 - \vec{v}_2|}|H_w|^2(2\pi)\delta(W - E_e - E_\nu)\frac{m_\nu}{(2\pi)^3}\frac{d^3p_\nu}{E_\nu}\frac{m_e}{(2\pi)^3}\frac{d^3p_e}{E_p} \tag{76}$$

where W, ignoring small momentum corrections, is the difference in (nuclear not atomic) masses, $2m_p - m_D \sim 0.931$ MeV. As we did previously in neutron β decay, we treat the amplitude in the allowed approximation and nucleon motion nonrelativistically. The Fermi operator connects only to the isospin analog state, that is, to the state identical to the initial state in terms of space and spin, but with $(T, M_T) = (T_i, M_{Ti} \pm 1)$ for β^- and β^+ decay, respectively. Now the reaction of interest, $p + p \to d + e^+ + \nu_e$, produces a final nuclear state with J = 1 and isospin T=0: this is an isospin singlet, so there is no corresponding state in p+p that can be reached by the Fermi operator. It follows that only the Gamow-Teller operator contributes. Using an earlier result for integration over the phase space, we find

$$\sigma = \frac{1}{|\vec{v}_1 - \vec{v}_2|}G_F^2\cos^2\theta_c\frac{1}{2\pi^3}\ |M_{GT}|^2\ \int_{m_e}^{W} F(Z,\epsilon)(W-\epsilon)^2\epsilon\sqrt{\epsilon^2 - m_e^2}\ d\epsilon \tag{77}$$

We can do the integral over the outgoing electron energy in β decay, ignoring the Coulomb correction for the outgoing electron in the field of the nucleus. This is a good approximation as the nuclear energy release in the decay, 0.931 MeV, means the outgoing electron and neutrino share .420 MeV of kinetic energy. If half of this goes to the electron on average, then the typical velocity of the electron is 0.7c. Thus

$$2\pi\eta = 2\pi Z_1 Z_2 \alpha/\beta \sim 0.065 \Rightarrow F(Z,\epsilon) \sim 0.97$$

So the Coulomb effects can be ignored. We find

$$\sigma = \frac{1}{|\vec{v}_1 - \vec{v}_2|} G_F^2 \cos^2\theta_c \frac{1}{2\pi^3} m_e^5 \left(\sqrt{x^2-1}(\frac{x^4}{30} - \frac{3x^2}{20} - \frac{2}{15}) + \frac{x}{4}\ln(x+\sqrt{x^2-1}) \right) |M_{GT}|^2 \tag{78}$$

where $x = W/m_e$.

Now we address the spin-isospin matrix element that appears in Eq. (78), as it is a bit different from the one we discussed for neutron β decay. Recall for the earlier case:

$$|M_{GT}|^2_{\rm neutron} \equiv \frac{g_A^2}{2J_i+1} |\langle J_f = 1/2; T_f = 1/2, M_{T_f} = 1/2 || \sigma\tau_+ || J_i = 1/2; T_i = 1/2, M_{T_i} = -1/2\rangle|^2 \tag{79}$$

This matrix element, reduced in angular momentum but not isospin, came from averaging over initial angular momentum states and summing over final, that is

$$\begin{aligned}
&\frac{1}{2}\left|\langle 1/2;\ 1/2,1/2||\sigma\tau_+||1/2;\ 1/2,-1/2\rangle\right|^2 = \\
&\frac{1}{2}\sum_{m_f,m,m_i} \langle 1/2,m_f;\ 1/2,1/2|\sigma_m\tau_+|1/2,m_i;\ 1/2,-1/2\rangle \\
&\qquad\qquad \times \langle 1/2,m_f;\ 1/2,1/2|\sigma_m\tau_+|1/2,m_i;\ 1/2,-1/2\rangle^\dagger = \\
&\frac{1}{2}\sum_{m_f,m,m_i} \left[(-1)^{1/2-m_f} \begin{pmatrix} 1/2 & 1 & 1/2 \\ -m_f & m & m_i \end{pmatrix}\right]^2 \left|\langle 1/2;\ 1/2,1/2||\sigma\tau_+||1/2;\ 1/2,-1/2\rangle\right|^2 = \\
&\qquad \frac{1}{2}\sum_m \frac{1}{3}\left|\langle 1/2;1/2,1/2||\sigma\tau_+||1/2;\ 1/2,-1/2\rangle\right|^2 = \\
&\qquad\quad \frac{1}{2}\left|\langle 1/2;\ 1/2,1/2||\sigma\tau_+||1/2;\ 1/2,-1/2\rangle\right|^2
\end{aligned} \tag{80}$$

The Gamow-Teller transition matrix element for p+p is a bit more complicated than in the case of the neutron: for the neutron, we had to specify only the initial and final spin and isospin. In contrast, the wave function of the $p+p$ initial state and the final-state deuteron can be written as a product of a center-of-mass piece and a relative wave function. For example, were we to ignore p-p interactions, the two-proton state could be decomposed

$$e^{i\vec{p}_1\cdot\vec{x}_1} e^{i\vec{p}_2\cdot\vec{x}_2} = e^{i(\vec{p}_1+\vec{p}_2)\cdot(\vec{x}_1+\vec{x}_2)/2} e^{i(\vec{p}_1-\vec{p}_2)\cdot(\vec{x}_1-\vec{x}_2)/2} \tag{81}$$

The first term is part of the integration that is done to generate the three-momentum-conserving delta function, $(2\pi)^3\delta^3(p_1+p_2-p_d-p_\nu-p_e)$, that was already employed in Eq. (76) to do the integral over the final-state deuteron's center-of-mass three-momentum. This part is analogous to the neutron. But for the two-nucleon system there remains a relative coordinate piece that, for simple plane waves is immediate

$$e^{i(\vec{p}_1-\vec{p}_2)\cdot(\vec{x}_1-\vec{x}_2)/2} \to \sqrt{4\pi} j_0(kr) Y_{00}(\Omega_r) \tag{82}$$

where $\vec{k} = (\vec{p}_1 - \vec{p}_2)/2$, $\vec{r} = (\vec{x}_1 - \vec{x}_2)$, and where we have retained only the s-wave contribution, which dominates at low energies. In a realistic case the relative wave function must be generated from solutions to the Schroedinger equation for bound and continuum states – as discussed below.

The relative p+p wave function differs from a plane wave due to the Coulomb barrier at larger separations and the strong interaction at short distance. To estimate the p+p rate we thus need to build a model for the relative wave function: we follow here the historical calculation of Bethe and Critchfield (though the derivation here differs in many of the details – and perhaps ought to be checked by the reader, as it is sufficiently complicated errors can easily creep in). It is worthwhile going through the details so that one can see how an S-factor is determined theoretically, in an important case where direct laboratory measurements are not possible. We also need to evaluate the spin/isospin matrix element. Since our radial wave function is s-wave, the spin is the angular momentum. We first do the spin/isospin matrix element (which interestingly Bethe and Critchfield did not address).

The deuteron is isoscalar and 95% s-wave: we will treat it as purely s-wave for this reason and because only this part of the wave function will connect to the very low energy p+p wave function, as this will be almost entirely s-wave. As the deuteron has T=0, and as the Pauli principle requires $L + S + T = 0$, the deuteron has$S = 1$, that is, the spin state is symmetric and the isospin state antisymmetric. The initial p+p state is isovector (symmetric) and as we have noted, is almost entirely $L = 0$.. Thus the only component of the initial spin state that contributes is the spin-antisymmetric component, $S = 0$. As the initial state corresponds to separated protons with uncorrelated spins, only the $S = 0$ component of that spin-uncorrelated wave function contributes.

In analogy with the second line of Eq. (80), the required matrix elements involves an average over initial proton spin magnetic quantum numbers and a sum over the final deuteron magnetic quantum numbers. The spin-part can be evaluated

$$|M_{GT}|^2_{pp\to d} = \frac{g_A^2}{2\cdot 2} \sum_{mp_1, m_{p_2}, m_d, m}$$

$$\langle \alpha_d; S = 1 m_d; T = 0, M_T = 0 | \sum_{i=1}^{2} \sigma(i)_m \tau_-(i) | \alpha_{pp}; 1/2 m_{p_1}, 1/2 m_{p_2}; T = 1 M_{T_i} = 1 \rangle$$

$$\times \langle \alpha_d; S = 1 m_d; T = 0, M_T = 0 | \sum_{i=1}^{2} \sigma(i)_m \tau_-(i) | \alpha_{pp}; 1/2 m_{p_1}, 1/2 m_{p_2}; T = 1 M_{T_i} = 1 \rangle^\dagger \quad (83)$$

where α_d and α_{pp} denote spatial quantum numbers of the $l = 0$ initial and final states. But the spin sums must yield an $S = 0$ initial state by antisymmetry, so we know the only contributing terms in the initial-state sum are

$$|1/2, m_{p_1} = 1/2; 1/2, m_{p_2} = -1/2\rangle =$$

$$\langle 1,0|1/2,1/2;1/2,-1/2\rangle\ |S=1,M_S=0\rangle + \langle 0,0|1/2,1/2;1/2,-1/2\rangle\ |S=0,M_S=0\rangle \rightarrow \frac{1}{\sqrt{2}}|S=0M_S=0\rangle$$

$$\text{and similarly } |1/2,m_{p_1}=-1/2;1/2,m_{p_2}=1/2\rangle \rightarrow \frac{1}{\sqrt{2}}|S=0M_S=0\rangle \tag{84}$$

Consequently

$$\begin{aligned} |M_{GT}|^2_{pp\rightarrow d} &= \frac{g_A^2}{4}\sum_{m,m_d}|\langle\alpha_d;1,m_d;0,0|\sum_{i=1}^{2}\sigma(i)_m\tau_-(i)|\alpha_{pp};0,0;1,1\rangle|^2 \\ &= \frac{g_A^2}{4}|\langle\alpha_d;1;0,0||\sum_{i=1}^{2}\sigma(i)\tau_-(i)||\alpha_{pp};0;1,1\rangle|^2 = \frac{3g_A^2}{2}|\langle\alpha_d|\alpha_{pp}\rangle|^2 \end{aligned} \tag{85}$$

The spin/isospin matrix element evaluation is easily evaluated by hand from the first line, simply by writing out the Pauli spinors and evaluating the corresponding Pauli spin matrix elements. In doing this, remember that the τ_- operator is defined as an isospin lowering operator (not a spherical one), giving unity when it lowers a proton to a neutron. In contrast, the σ_m are the spherical projections of the Pauli spin matrices, defined as $\sigma_m = \hat{e}_m\cdot\vec{\sigma}$, where the spherical unit vectors are defined by $\hat{e}_0 = \hat{e}_z$ and $\hat{e}_{\pm1} = \mp(\hat{e}_x \pm i\hat{e}_y)/\sqrt{2}$. The hand calculation gives $-\sqrt{6}$ for the spin/isospin matrix element, using the first line above. Alternatively, one can apply the Ikeda (Gamow-Teller) sum rule to the second line, which involves the difference in the beta decay strengths and can be written when Z≥N as

$$\frac{1}{2J_i+1}\left[\sum_f|\langle f||\sum_i\sigma(i)\tau_-(i)||i\rangle|^2 - \sum_f|\langle f||\sum_i\sigma(i)\tau_+(i))||i\rangle|^2\right] = 3(Z-N) \tag{86}$$

to write down the answer by inspection. In this case, the τ_+ operator annihilates our two-proton initial state, so only the τ_- term contributes. We have $J_i = S_i = 0$, and the final state on the left is the only one that connects to the initial state, given that we consider only $l = 0$ states. Consequently the needed reduced spin-isopsin matrix element must be 6.

Similarly, the angular integral is just unity, by the orthogonality of the Y_{lm}s. Thus our expression reduces to

$$\sigma = \frac{1}{|\vec{v}_1-\vec{v}_2|}G_F^2\cos^2\theta_c\frac{3g_A^2}{4\pi^3}m_e^5\left(\sqrt{x^2-1}(\frac{x^4}{30}-\frac{3x^2}{20}-\frac{2}{15})+\frac{x}{4}\ln(x+\sqrt{x^2-1})\right) \times \left|\int r^2drR_d^{0*}(r)R_{pp}^0(r)\right|^2 \tag{87}$$

So the remaining task is to evaluate the radial wave functions and determine the needed overlap.

We begin by specifying a simple model that nevertheless has enough flexibility to reproduce important feature of the two-nucleon system, such as the binding energy $E_b = 2.22$ MeV of the deuteron. (Note that E_b is defined as positive.) We solve the 3D square well problem for a bound n+p system,

$$R_d^{l=0}(r)Y_{00}(\Omega_r) \equiv \frac{\chi_d}{r}Y_{00}(\Omega_r) \tag{88}$$

$$\begin{cases} \left[-\frac{1}{2\mu}\frac{d^2}{dr^2} + |E_b| - V_t\right]\chi_d = 0 & r < R_N \\ \\ \left[-\frac{1}{2\mu}\frac{d^2}{dr^2} + |E_b|\right]\chi_d = 0 & r > R_N \end{cases} \Rightarrow$$

$$R_d^0(r) = A_0 \begin{cases} \frac{1}{ar}\sin(ar) & r < R_N \\ \\ \frac{1}{ar}e^{-b(r-R_N)}\sin(aR_N) & r > R_N \end{cases}$$

$$\text{eigenvalue condition} \quad : \quad \cot(aR_N) = -\frac{b}{a}$$

$$A_0 = \frac{a^2}{\sin(aR_N)}\left[2\mu|E_b|\right]^{1/4}\left[\frac{1}{2\mu V_t}\right]^{1/2}\left[\frac{2}{1+bR_N}\right]^{1/2}$$

where $a = \sqrt{2\mu(V_t - |E_b|)}$, $b = \sqrt{2\mu|E_b|}$, $\mu = m_p/2$, and R_N and $V_t = |V_t|$ are the radius and depth of the spherical square well. Here the subscript "t" denotes that we are working in the triplet channel, that is, S=1 (and thus T=0 as L=0). This is the NN channel that has a bound state. For example, the choice V=50 MeV and $R_N = 1.66$ f would give the correct deuteron binding energy and thus the correct bound-state tail. (We will discuss later how we fine tune V and R_N.)

Similarly, we need to solve the 3D square well + Coulomb problem for the p+p system. This is the singlet channel, S=0, with L=0 and T=1. (L+S+T must be odd to produce an antisymmetric wave function.) We know there is no bound state in this channel, so we anticipate the potential will be less deep than in the triplet case. (We return to this point later.) We assume the Coulomb potential outside of R_N, and our square well inside. For simplicity, we take the same radius for the triplet and singlet channels. This yields,

$$R_{pp}^{l=0}(r)Y_{00}(\Omega_r) \equiv \frac{\chi_{pp}}{r}Y_{00}(\Omega_r) \tag{89}$$

$$\begin{cases} \left[-\frac{1}{2\mu}\frac{d^2}{dr^2} - E - V_s\right]\chi_{pp} = 0 & r < R_N \\ \\ \left[-\frac{1}{2\mu}\frac{d^2}{dr^2} - E + \frac{\alpha}{r}\right]\chi_{pp} = 0 & r > R_N \end{cases} \Rightarrow$$

$$R_{pp}^0(r) = \begin{cases} B_0\frac{1}{gr}\sin(gr) & r < R_N \\ \\ \sqrt{4\pi}\frac{e^{i\delta}\cos\delta}{kr}\left[F_0(\eta, kr) + \tan\delta G_0(\eta, kr)\right] & r > R_N \end{cases}$$

where $g = \sqrt{2\mu(V_s + E)}$, $\eta = \alpha Z_1 Z_1 \mu/k = \alpha\mu/k$, and $E = k^2/2\mu$. As we will see explicitly

below, we could set $e^{i\delta}\cos\delta \to 1$ as the phase shift is very small for the energies of interest, but we will retain it to remain exact. In contrast to the bound-state case, the asymptotic normalization of the outgoing solution is fixed by our plane-wave normalization condition for scattering, so that B_0 of the interior wave function is determined by matching (compare Eq. (82)). Matching of the log derivatives of the interior and exterior solutions at R_N then determines δ.

The calculation can be simplified by using the Clifford-Bessel expansion for the Coulomb wavefunctions (see Abramowitz and also Froberg, RMP 27 (1955) 399). This expansion is particular attractive in that it isolates the dependence on E by utilizing the parameter $2\eta\rho$, where we define $\rho = kr$ and $\rho_N = kR_N$, which is independent of energy. Thus one can do a power series expansion in E relatively simply with this expansion – an elaboration of the current calculation that we will tackle as a class project, possibly. To lowest order the expansion gives

$$\begin{aligned} F_0(\eta,\rho) &= C_0(\eta)\sqrt{\frac{\rho}{2\eta}}\left[I_1(2\sqrt{2\eta\rho}) + O(E)\right] \\ F_0'(\eta,\rho) &= C_0(\eta)\left[I_0(2\sqrt{2\eta\rho}) + O(E)\right] \\ G_0(\eta,\rho) &= \frac{1}{C_0(\eta)} 2\sqrt{2\eta\rho}\left[K_1(2\sqrt{2\eta\rho}) + O(E)\right] \\ G_0'(\eta,\rho) &= -\frac{1}{C_0(\eta)} 4\eta\left[K_0(2\sqrt{2\eta\rho}) + O(E)\right] \end{aligned} \tag{90}$$

Here $F_0'(\eta,\rho) \equiv d/d\rho\ F_0(\eta,\rho)$, the Ks and Is are the usual Bessel functions, and $C_0(\eta)^2 = 2\pi\eta/(e^{2\pi\eta}-1)$. While there are many approximations for Coulomb functions, this one as an expansion in E preserves derivatives (many other approximation schemes do not). After completing the necessary algebra and simplifying one finds from matching wave functions and derivatives at R_N, one finds

$$\tan\delta = C_0(\eta)^2\ \rho_N\ \lambda(gR_N,\eta\rho_N) \quad \text{where}$$

$$\lambda(gR_N,\eta\rho_N) = \frac{\sqrt{2\eta\rho_N}\ I_0(2\sqrt{2\eta\rho_N}) - (gR_N\cot gR_N)\ I_1(2\sqrt{2\eta\rho_N})}{(gR_N\cot gR_N)4\eta\rho_N\ K_1(2\sqrt{2\eta\rho_N}) + 2(2\eta\rho_N)^{3/2}\ K_0(2\sqrt{2\eta\rho_N})} \tag{91}$$

Note that if we approximate $g = \sqrt{2\mu(V_s+E)} \sim \sqrt{2\mu V_s}$, which is a very good approximation, λ is independent of energy. (Alternatively one could do a power series expansion, were one very interested in the energy dependence of S(E) In fact, I think a nice effective range expansion for $k\cot\delta$ would result from doing this and from including higher-order Clifford-Bessel expansion terms.) The normalization of the interior wave function is also found

$$\begin{aligned} B_0 &= \sqrt{4\pi}e^{i\delta}\cos\delta\ \frac{g}{k}\ \frac{F_0(\eta,\rho_N)+\tan\delta G_0(\eta,\rho_N)}{\sin gR_N} \\ &= \sqrt{4\pi}e^{i\delta}\cos\delta\frac{gR_N}{\sin gR_N}C_0(\eta)\left[\frac{1}{\sqrt{2\eta\rho_N}}I_1(2\sqrt{2\eta\rho_N}) + 2\sqrt{2\eta\rho_N}\ \lambda\ K_1(2\sqrt{2\eta\rho_N})\right] \end{aligned} \tag{92}$$

From these results, with some rearrangement, one can write the pp solution

$$R_{pp}(r) = \sqrt{4\pi}e^{i\delta}\cos\delta C_0(\eta)\begin{cases} \frac{R_N}{r}\frac{\sin gr}{\sin gR_N}\left[\frac{1}{\sqrt{2\eta\rho_N}}I_1(2\sqrt{2\eta\rho_N}) + 2\lambda\sqrt{2\eta\rho_N}K_1(2\sqrt{2\eta\rho_N})\right] & r \le R_N \\ \frac{1}{\sqrt{2\eta\rho}}I_1(2\sqrt{2\eta\rho}) + \frac{R_N}{r}2\lambda\sqrt{2\rho\eta}K_1(2\sqrt{2\eta\rho}) & r \ge R_N \end{cases} \tag{93}$$

We can now break up the integral appearing in Eq. (87) into two parts

$$\int_0^\infty r^2 dr R_d^*(r)R_{pp}(r) = \int_0^{R_N} r^2 dr R_d^*(r)R_{pp}(r) + \int_{R_N}^\infty r^2 dr R_d^*(r)R_{pp}(r) \tag{94}$$

The first integral can be done analytically, yielding

$$\int_0^{R_N} r^2 dr R_d^*(r)R_{pp}(r) = \sqrt{8\pi}e^{i\delta}\cos\delta\ C_0(\eta)$$
$$\times\frac{[2\mu E_b]^{1/4}}{2\mu(V_s - V_t + E + E_b)}\left[\frac{V_t - E_b}{V_t}\right]^{1/2}\left[\frac{1}{1+\sqrt{2\mu E_b R_N^2}}\right]^{1/2}\Lambda_I \tag{95}$$

where

$$\Lambda_I \equiv \left[\frac{1}{\sqrt{2\eta\rho_N}}I_1(2\sqrt{2\eta\rho_N}) + 2\lambda\sqrt{2\eta\rho_N}K_1(2\sqrt{2\eta\rho_N})\right]$$
$$\times\left[\sqrt{2\mu(V_t - E_b)R_N^2}\cot\sqrt{2\mu(V_t - E_b)R_N^2} - \sqrt{2\mu(V_s + E)R_N^2}\cot\sqrt{2\mu(V_s + E)R_N^2}\right] \tag{96}$$

The second integral requires a numerical integration (or some expansion, which is what Bethe and Critchfield did).

$$\int_{R_N}^\infty r^2 dr R_d^*(r)R_{pp}(r) = \sqrt{8\pi}e^{i\delta}\cos\delta\ C_0(\eta)\frac{1}{[2\mu E_b]^{3/4}}\left[\frac{V_t - E_b}{V_t}\right]^{1/2}\left[\frac{1}{1+\sqrt{2\mu E_b R_N^2}}\right]^{1/2}\Lambda_O$$
$$\text{where}\ \ \Lambda_O \equiv \left[2\mu E_b R_N^2\right]^{1/4}\int_{\sqrt{2\mu E_b R_N^2}}^\infty \sqrt{y}dy\ e^{-(y-\sqrt{2\mu E_b R_N^2})}$$
$$\times\left[\frac{1}{\sqrt{2\eta\rho_N}}I_1\left(2\sqrt{y}\frac{[2\eta\rho_N]^{1/2}}{[2\mu E_b R_N^2]^{1/4}}\right) + 2\lambda\sqrt{2\eta\rho_N}K_1\left(2\sqrt{y}\frac{[2\eta\rho_N]^{1/2}}{[2\mu E_b R_N^2]^{1/4}}\right)\right] \tag{97}$$

Except for an extremely small E dependence hiding in λ, Λ_0 is energy independent.

We can now plug back into our original cross section formula and do a bit of algebra to find

$$\sigma = \sqrt{\frac{\mu}{2E}}G_F^2\cos^2\theta_c\frac{6g_A^2}{\pi^2}m_e^5\left[\sqrt{x^2-1}(\frac{x^4}{30} - \frac{3x^2}{20} - \frac{2}{15}) + \frac{x}{4}\ln(x+\sqrt{x^2-1})\right]\cos^2\delta C_0^2(\eta)$$
$$\times\frac{1}{[2\mu E_b]^{3/2}}\left[\frac{V_t - E_b}{V_t}\right]\left[\frac{1}{1+\sqrt{2\mu E_b R_N^2}}\right]\left[\frac{E_b}{V_s - V_t + E + E_b}\Lambda_I + \Lambda_O\right]^2 \tag{98}$$

S(0), the zero-energy S-factor, is defined by taking the limit as $E \to 0$ of $E\ e^{2\pi\eta}\ \sigma(E)$. Thus doing this and simplifying, we find our final answer

$$S_{pp}(0) = G_F^2 \cos^2\theta_C \frac{3g_A^2}{\pi} \alpha m_e^5 M_N \frac{1}{[2\mu E_b]^{3/2}} \left[\frac{V_t - E_b}{V_t}\right] \left[\frac{1}{1+\sqrt{2\mu E_b R_N^2}}\right]$$
$$\left[\sqrt{x^2-1}(\frac{x^4}{30} - \frac{3x^2}{20} - \frac{2}{15}) + \frac{x}{4}\ln(x+\sqrt{x^2-1})\right] \left[\frac{E_b}{V_s - V_t + E_b}\Lambda_I + \Lambda_O\right]^2 \tag{99}$$

Note the dimensions 1/mass, so we evaluate everything in MeV units, then multiply by $(\hbar c)^2$= (197.3 MeV f)^2 to get the final dimensions. Thus all the dust has cleared except for the numerical evaluation. Also note the dependence of the deuteron binding energy, which defines an important length scale: the smaller E_b, the larger the S-factor.

Now we come to the question of the specific parameters to use for our strong potentials. Our approach is a bit of a poor-man's effective theory: we know that the long-wavelength behavior of the problem is crucial, so we adopt a model that, while simple, still incorporates the most important aspects of the infrared physics. Specifically in the singlet (unbound) channel we would like to build in good long-behavior behavior at low E, which means trying to reproduce experimental values for parameters like the singlet scattering length and effective range,

$$k\cot\delta_s = -\frac{1}{a^s} + \frac{1}{2}r_0^s k^2 + ... \tag{100}$$

In the deuteron triplet (S=1) channel the crucial parameters are the deuteron binding energy, since this governs the wave function tail, as the low-energy scattering parameters analogous to those above. Our model is limited because we have only three parameters, R_N, V_s and V_t.

We start in the deuteron channel and fit R_N and V_t to yield the correct binding energy of E_b=2.22 MeV and scattering length of $a^t = 5.418$ f. The former constraint is just that we must satisfy the eigenvalue equation,

$$\cot aR_N = -b/a \quad \Rightarrow \quad \cot\sqrt{2\mu(V_t - E_b)R_N^2} = \sqrt{\frac{E_b}{V_t - E_b}} \tag{101}$$

As we are not considering charge-symmetry-breaking strong interaction effects, the singlet strong-interaction two-proton, proton-neutron, and two neutron problems are the same. Thus there is no need to clutter up the second constraint with Coulomb effects. We solve the square well problem and evaluate $\tan\delta$ as $k \to 0$ to find

$$\tan\delta \to kR_N \left[\frac{1 - \sqrt{2\mu V_t R_N^2}\cot 2\mu V_t R_N^2}{\sqrt{2\mu V_t R_N^2}\cot 2\mu V_t R_N^2}\right] \equiv -ka^t \tag{102}$$

Using Mathematics FindRoot to simultaneous solve the above two equations yields

$$V_t = 33.54\text{MeV} \qquad R_N = 2.107\text{ f} \tag{103}$$

We retain the same radius for the singlet channel, but find the V_s that gives the anomalous scattering length $a^s = -23.727$ f (which indicates there is no bound state, but there is a resonance very close to threshold). Fitting V_s to a^s yields

$$V_s = 21.502 \text{ MeV} \tag{104}$$

And we note our model is not perfect. We can easily evaluate the effective ranges, finding $r_o^t = 1.772$ f (1.833 f) and $r_o^s = 2.183$ f (2.67 f), where the experimental values are given in parenthesis. So now we can do our integrals (doing Λ_O numerically on Mathematica), yielding

$$\frac{E_b}{V_s - V_t + E_b}\Lambda_I = 1.138 \quad \Lambda_O = 4.543, \tag{105}$$

so we find most of the integral comes from outside the nuclear range. Plugging these numbers into Eq. (99) then yields

$$S_{pp}(0) = 5.81 \times 10^{-23} \text{ MeV f}^2 = 5.81 \times 10^{-25} \text{ MeV barns}. \tag{106}$$

The currently accepted value is $4.01(1 \pm 0.009) \times 10^{-25}$ MeV barns. Thus our value is 50% higher. The consistency can be tested by altering our nuclear model over a reasonable range. For example, were we to adopt $V_t \sim 50$ MeV, a not unreasonable value if one looks at schematic models, and fit only the deuteron eigenvalue, then we would deduce $R_N \sim 1.661$ f. The scattering length and effective range are a bit off, but not unreasonable, 5.180 f and 1.444 f, respectively. We fit a_o^s to obtain $V_s = 35.09$ MeV, and predict $r_o^s \sim 1.708$. We find $E_b\Lambda_I/(V_s - V_t + E_b) = 0.476$ and $\Lambda_O = 3.159$, and $S(0) \sim 2.65 \times 10^{-25}$ MeV barns. This is $\sim 50\%$ too low. Thus we argue we are in the ballpark.

In a true effective theory calculation, one would have to worry about the operator as well. There is a short-range two-nucleon correction that requires the fixing of one low-energy constant, called L_{1A}, that yields about a 5% correction.

It would be quite interesting to embellish this calculation, to see if one can do better. A more complicated square-well potential that included a repulsive hard core would introduce needed parameters that could then be used to "mock-up" the low energy behavior: V_t^{HC}, V_t, R_N, R_N^{HC}, V_s^{HC}, and V_s could be fit to the effective range expansion up through order k^4 in both the singlet and triplet channels. The primary motivation for this would be to determine $S'(0)$ and $S''(0)$. The literature gives a result for $S'(0)$,

$$\lim_{E \to 0} \frac{dS_{pp}(E)}{dE} \sim S_{pp}(0)(11.2 \pm 0.1) \text{ MeV}^{-1} \tag{107}$$

Thus at 10 keV, this slope generates a $\sim 10\%$ correction to the S-factor.

Now that we know the S-factor, we can plug it into our rate formula to determine the rate of the p+p reaction. Recall

$$\frac{E_o}{kT} \sim \left(\frac{\pi\alpha Z_1 Z_2}{\sqrt{2}}\right)^{2/3} \left(\frac{\mu c^2}{kT}\right)^{1/3} \sim \frac{5.23}{T_7^{1/3}} \tag{108}$$

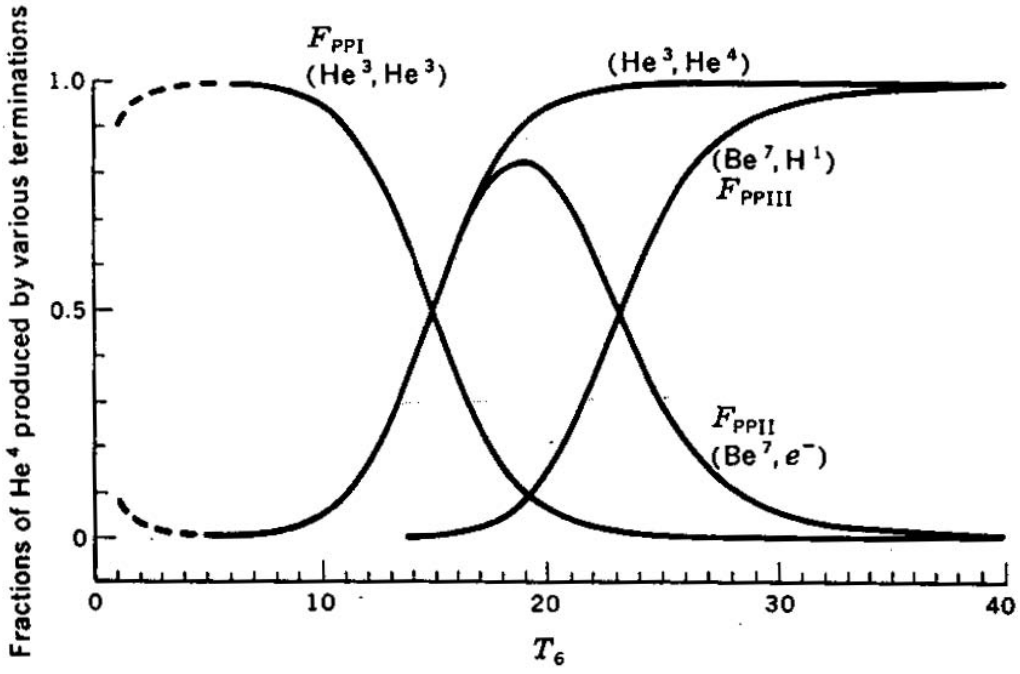

Figure 9: The fractions of ^{4}He contributed by the ppI, ppII, and ppIII cycles as a function of stellar temperature.

So in the core of the sun, where $T_7 \sim 1.5$, $E_o/kT \sim 4.57$ and $E_o \sim 5.9$ keV, the most effective energy for the p+p reaction. The rate formula then gives

$$r_{pp} = N_p^2 \; 7.1 \times 10^{-38} \mathrm{cm}^3/\mathrm{sec} \; e^{-15.7 T_7^{-1/3}} T_7^{-2/3} \sim N_p^2 \; 5.9 \times 10^{-44} \mathrm{cm}^3/\mathrm{sec} \tag{109}$$

Now the number density at the center of the sun is about $3 \times 10^{25}/\mathrm{cm}^3$, so $r_{pp} \sim 0.5 \times 10^8/\mathrm{cm}^3/\mathrm{sec}$. The time scale for burning hydrogen is the number density divided by twice the burning rate (two protons are consumed per reaction)

$$\tau_{\mathrm{sun}} \sim 8.6 \mathrm{b.y} \tag{110}$$

which can be compared to the sun's present age, 4.55 b.y. Thus it has lived about half its lifetime.

If the initiating p+p β decay reaction occurs, we can see relatively easily how the rest of the burning might proceed,

$$d + p \rightarrow {}^3\mathrm{He} + \gamma \quad \text{followed by} \quad {}^3\mathrm{He} + {}^3\mathrm{He} \rightarrow {}^4\mathrm{He} + p + p \tag{111}$$

This is called the ppI cycle and is, indeed, the most robost part of the pp chain in stars with temperatures like our sun: about 84% of the ^{4}He produced today in the solar core is predicted to be synthesized in this way. The two reactions above are of the type we have previously discussed. We could use the Lane-Emden polytrope stellar model and add to it the network reactions

$$p + p \rightarrow d + e^+ + \nu_e \quad r_{pp} \sim \lambda_{pp} \frac{N_p^2}{2}$$

$$d + p \rightarrow {}^3\mathrm{He} + \gamma \quad r_{pd} \sim \lambda_{pd} N_p N_d$$

$${}^3\mathrm{He} + {}^3\mathrm{He} \rightarrow {}^4\mathrm{He} + p + p \quad r_{33} \sim \lambda_{33} \frac{N_{3\mathrm{He}}^2}{2}$$

Here r represents a rate and $\lambda = \langle \sigma v \rangle$. From one calculated S-factor (for pp) and two that are measured, we could calculate the production of He once the composition and temperature of our volume of interest was specified.

One feature of interest in this simple network is that d and ^{3}He both act as "catalysts": they are produced and then consumed in the burning. In a steady state process, this implies they must reach some equilibrium abundance where the production rate equals the destruction rate. That is, the general rate equation

$$\frac{dN_d}{dt} = \lambda_{pp} \frac{N_p^2}{2} - \lambda_{pd} N_p N_d \tag{112}$$

is satisfied at equilibrium by replacing the LHS by zero. Thus

$$\left(\frac{N_p}{N_d} \right)_{\mathrm{equil}} = \frac{2\lambda_{pd}}{\lambda_{pp}} \tag{113}$$

But from the S-factors

$$S_{12}(0) = 2.5 \cdot 10^{-4} \text{ kev b} \quad S_{11}(0) = 4.01 \cdot 10^{-22} \text{ kev b} \tag{114}$$

and our rate formula

$$\lambda_{12} = (7.21 \cdot 10^{-19} \text{cm}^3/\text{sec}) \frac{1}{A Z_1 Z_2} \left[\frac{S(E_o)}{\text{kev} - \text{b}} (Z_1^2 Z_2^2 A)^{2/3} (\frac{19.7}{T_7^{1/3}})^2 e^{-(Z_1^2 Z_2^2 A)^{1/3} 19.7/T_7^{1/3}} \right] \tag{115}$$

We can plug in the values

$$p + p: \quad Z_1 = Z_2 = 1 \quad A = 1/2$$

$$p + d: \quad Z_1 = Z_2 = 1 \quad A = 2/3$$

to find

$$\left(\frac{N_p}{N_d} \right)_{\text{equil}} = (0.9 \cdot 10^{-18}) e^{1.574/T_7^{1/3}} \tag{116}$$

Therefore this ratio is a decreasing function of T_7: the higher the temperature, the lower the equilibrium abundance of deuterium. Therefore in the region of the sun where the ppI cycle is operating, the deuterium abundance is lowest in the sun's center. Plugging in the solar core temperature

$$T_7 = 1.5 \Rightarrow \left(\frac{N_d}{N_p} \right) = 3.6 \cdot 10^{-18} \tag{117}$$

There isn't much deuterium about: using $N_p \sim 3 \cdot 10^{25}/\text{cm}^3$ one finds $N_d \sim 10^8/\text{cm}^3$. Remembering our previous result

$$r_{pp} \sim 0.6 \times 10^8/\text{cm}^3/\text{sec} \tag{118}$$

it follows that the typical life time of a deuterium nucleus is $\tau_d \sim 1$ sec. That is, deuterium is burned instantaneously and thus reaches equilibrium very, very quickly.

This result then allows us to write the analogous equation for ^{3}He as

$$\frac{dN_3}{dt} = \lambda_{pp} \frac{N_p^2}{2} - 2\lambda_{33} \frac{N_3^2}{2} \tag{119}$$

where the factor of two in the term on the right comes because the ^{3}He+^{3}He reaction destroys two ^{3}He nuclei. Thus at equilibrium

$$\left(\frac{N_3}{N_p} \right)_{\text{equil}} = \sqrt{\frac{\lambda_{pp}}{2\lambda_{33}}} \tag{120}$$

Using $S_{33}(0) = 5.15 \cdot 10^3$ keV b we can again do the rate algebra to find

$$\left(\frac{N_3}{N_p} \right)_{\text{equil}} = (1.33 \cdot 10^{-13}) e^{20.65 T_7^{-1/3}} = \begin{pmatrix} 9.08 \cdot 10^{-6} & T_7 = 1.5 \\ 1.24 \cdot 10^{-4} & T_7 = 1.0 \end{pmatrix} \tag{121}$$

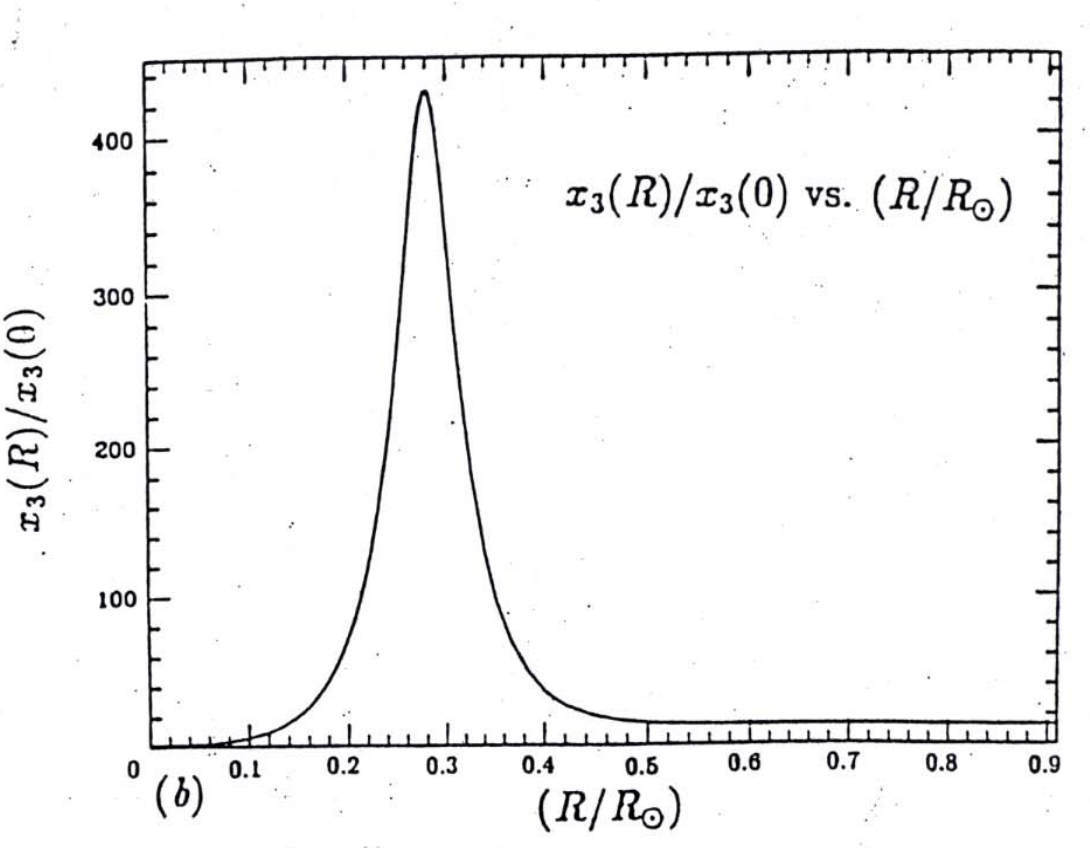

Figure 10: The distribution of ^{3}He in the sun, showing a sharp gradient in this element, which acts like a catalyst in the pp chain. The equilibrium abundance and the time required to reach equilibrium are both sharply decreasing functions of T – larger in the cooler parts of the sun. But at large radii, beyond $0.3R_o$, the abundance has not yet reached equilibrium.

This ratio is clearly a sharply decreasing function of T_7 and thus a sharply increasing function of r. That is, a sharp gradient in ^{3}He is established in the sun.

One can estimate the time required to reach equilibrium in a simple way: as the burning of ^{3}He is quadratic in the abundance, it will not become significant until one is rather close to the ^{3}He equilibrium value. Thus a reasonable estimate of the time require to get close (say a factor of 2) to equilibrium is just the time required to produce the requisite number of ^{3}He nuclei. At the sun's center, we have found that the ^{3}He abundance is $(9.08 \cdot 10^{-6})(4.5 \cdot 10^{25}/\mathrm{cm}^3) = 4.1 \cdot 10^{20}/\mathrm{cm}^3$, where we have assumed 75% of the matter is protons (as it was when the sun first entered the main sequence). Thus

$$\tau_{^3\mathrm{He}} \sim (4.1 \cdot 10^{20})/(1.3 \cdot 10^{8})\mathrm{sec} \ \sim 10000 \text{ years} \tag{122}$$

The same calculation at $T_7 \sim 1.0$, where a reasonable solar density of 36 g/cm^3 and a 75% proton abundance is used, gives

$$\begin{aligned} r_{pp} &\sim 3.0 \times 10^6/\mathrm{cm}^3/\mathrm{sec} \\ N_3 &\sim 2 \times 10^{21}/\mathrm{cm}^3 \\ \Rightarrow \tau_{^3\mathrm{He}} &\sim 21\mathrm{M.y.} \end{aligned} \tag{123}$$

It turns out that at temperatures of $T_7 \sim .65$, the equilibration time corresponds to the present age of the sun. This temperature characterizes a solar radius of about 0.27, at the very edge of the energy-producing core. The resulting interesting profile of ^{3}He is shown in the figure.

There are some interesting issues connected with this ^{3}He gradient. It was shown by Dilke and Gough that it implies the sun is overstable to large-amplitude radial oscillations. If one throws a ^{3}He rich volume element towards the core, the ^{3}He will ignite at the higher temperatures, become bouyant, and return to its original equilibrium position with a kinetic energy greater than the required for the original perturbation. This has lead to speculations that the ^{3}He gradient could trigger sudden overturn of the core. Most of the experts believe there is no large amplitude trigger that will allow the sun to discover the existence of this instability.

To be somewhat more complete, the initial step of the ppI cycle can occur in a different way

$$p + p + e^- \rightarrow d + \nu_e \tag{124}$$

But the electron capture process only accounts for about 1% of the pp reactions. Thus the full ppI cycle can be written

$$\begin{aligned} p + p \rightarrow d + e^+ + \nu_e \quad \text{or} \quad & p + p + e^- \rightarrow d + \nu_e \\ d + p \ &\rightarrow \ ^3\mathrm{He} + \gamma \\ ^3\mathrm{He} + {}^3\mathrm{He} \ &\rightarrow \ ^4\mathrm{He} + p + p \qquad \text{ppI cycle} \end{aligned} \tag{125}$$

However there are two other paths through the pp chain that can occur if ^{3}He burns by another path. Thus

$$^3\mathrm{He} + {}^3\mathrm{He} \rightarrow {}^4\mathrm{He} + p + p \quad \text{vs.} \quad {}^3\mathrm{He} + {}^4\mathrm{He} \rightarrow {}^7\mathrm{Be} + \gamma$$

determines the ppI vs. ppII+ppIII splitting. The splitting between the ppII and ppIII cycles depends on the fate of the ^{7}Be

$$^7\mathrm{Be} + e^- \rightarrow {}^7\mathrm{Li} + \nu \quad \text{vs.} \quad {}^7\mathrm{Be} + p \rightarrow {}^8\mathrm{B} + \gamma.$$

Thus the two additional cycles are

$$\begin{aligned} p + p \rightarrow d + e^+ + \nu_e \quad \text{or} \quad p + p + e^- \rightarrow d + \nu_e \\ d + p &\rightarrow {}^3\mathrm{He} + \gamma \\ {}^3\mathrm{He} + {}^4\mathrm{He} &\rightarrow {}^7\mathrm{Be} + \gamma \\ {}^7\mathrm{Be} + e^- &\rightarrow {}^7\mathrm{Li} + \nu_e \\ {}^7\mathrm{Li} + p &\rightarrow 2\,{}^4\mathrm{He} \qquad \text{ppII cycle} \end{aligned} \tag{126}$$

and

$$\begin{aligned} p + p \rightarrow d + e^+ + \nu_e \quad \text{or} \quad p + p + e^- \rightarrow d + \nu_e \\ d + p &\rightarrow {}^3\mathrm{He} + \gamma \\ {}^3\mathrm{He} + {}^4\mathrm{He} &\rightarrow {}^7\mathrm{Be} + \gamma \\ {}^7\mathrm{Be} + p &\rightarrow {}^8\mathrm{B} + \gamma \\ {}^8\mathrm{B} &\rightarrow {}^8\mathrm{Be} + e^+ + \nu_e \\ {}^8\mathrm{Be} &\rightarrow 2\,{}^4\mathrm{He} \qquad \text{ppIII cycle} \end{aligned} \tag{127}$$

The calculations presented below will show that the competition between the three cycles is quite sensitive to the interior temperature of the sun, and to core composition. We also note that, in principle, we can experimentally determine the relative importance of the three cycles: the cycles are distinguished by the neutrinos they produce.

$$\text{ppI} + \text{ppII} + \text{ppIII rate} \;\propto\; \Phi_\nu(pp) : \beta \text{ endpoint} \;\sim 0.420 \text{ MeV}$$

$$\text{ppII rate} \;\propto\; \Phi_\nu({}^7\mathrm{Be}) : \text{ electron capture, } E_\nu = 0.86 \text{ MeV}(90\%),\ 0.38 \text{ MeV}(10\%)$$

$$\text{ppIII rate} \;\propto\; \Phi_\nu(8\mathrm{B}) : \beta \text{ endpoint} \;\sim 15\text{MeV}$$

• The ^{3}He+^{3}He $\leftrightarrow$ ^{3}He+^{4}He branching:
The Coulomb effects for these two reactions are rather similar, except for small effects proportional to the different masses. The heavier nucleus moves more slowly, and thus is at a disadvantage in overcoming Coulomb barriers. The S-factor for the 3+3 reaction is larger than that for the 3+4 reaction by almost a factor of 10^4. However we have also seen that

the core ambundance of ^{3}He is almost a factor of 10^5 less than that of ^{4}He. The net result, from our rate formulas, is

$$\left(\frac{r_{34}}{r_{33}}\right)_{\rm equil} = 2\left(\frac{N_p}{N_3}\right)_{\rm equil}\left(\frac{N_4}{N_p}\right) 1.85\cdot 10^{-4}\frac{S_{34}(E_o)}{\text{kev b}}e^{-2.5T_7^{-1/3}}$$

Noting that

$$\left(2\frac{N_p}{N_3}\right)_{\rm equil} = 1.5\cdot 10^{13}e^{-20.65T_7^{-1/3}}$$

and using $S_{34}\sim 0.52$ keV b leads to

$$\frac{r_{34}}{r_{33}} \sim 3.6\cdot 10^8 e^{-23.15T_7^{-1/3}}$$

It is clear that higher temperatures favor the ppII+ppIII cycles. We can solve for the temperature where the ratio becomes 1,

$$T_7^{\rm critical}\sim 1.62$$

Thus the 3+3 reaction dominates at solar temperatures, but not in stars that are $\sim 10\%$ hotter. At the center of the sun, where $T_7\sim 1.5$, the ratio is 0.6; at $T_7\sim 1.2$, corresponding to a radius half way through the energy producing core, the ratio is 0.12. The figure, from Cameron, shows the ppI/ppII+ppIII branching as a function of T_7.

The next issue is the branching ratio between the reactions that determine the ppII - ppIII splitting,

$$^7\text{Be}+e^-\rightarrow {}^7\text{Li}+\nu \quad\Leftrightarrow\quad {}^7\text{Be}+p\rightarrow {}^8\text{B}+\gamma$$

Two observations about the first reaction are

• For terrestrial atoms, the electron capture rate is measured and corresponds a lifetime of

$$\tau_{1/2}^{lab}\sim 53 \text{ days}$$

• Electron capture is a weak interaction, so it is effectively a contact interaction with the nucleus. Therefore the rate is proportional to the probability to find an electron at the nucleus. For a terrestrial light atom, the electron states with strong overlab with the nucleus are the $1s_{1/2}$ orbits. Thus the terrestrial rate above must represent that from the two $1s_{1/2}$ orbits. However in the sun, $kT\sim 1$ keV while the $1s_{1/2}$ binding energy in ^{7}Be is Z^2 13.6 eV ~ 0.22 keV; the comparison for p and ^{4}He is less favorable. Thus most of the solar electrons must be in the plasma: we expect continuum capture of electrons to be a very important part of the solar ^{7}Be electron capture.

This seems to argue that we can make a good estimate of the solar electron capture rate by scaling the terrestrial rate to the ratio of electron densities (at the nucleus) for the sun and for a terrestrial atom. That is,

$$\omega^{\rm solar}\sim \omega^{\rm terrestrial}\frac{|\Psi_{\rm solar}(r=0)|^2}{|\Psi_{\rm terrestrial}(r=0)|^2}$$

Now we can estimate the denominator by using the Bohr atom estimate for the 1s probability: this is quite a reasonable approximation even for a 4-electron atom because the 1s electrons are close to the nucleus and basically see just the nuclear charge. The result is

$$2|\Psi_{1s}(0)|^2 \sim 2\frac{(Z\alpha m_e c^2)^3}{\pi(\hbar c)^3} \sim |\Psi_{\rm terrestrial}(r=0)|^2$$

We also can estimate the numerator in a straight-forward way. Suppose our overall solar density of electrons is denoted N_e. Just as we earlier argued in calculating the pp S-factor, most of the time the electrons are well away the nucleus (and other electrons) and behave as plane waves, with some standard uniform density. Thus the density at the nucleus is just the average density, multiplied by the Coulomb penetration (which gives the ratio of the electron probability at the nucleus to that at large r). For electron-nucleus interactions, the Coulomb potential is attractive. Thus the electron wave function is sucked into the nucleus: the nuclear electron density is *higher* that the average density. But we know the form of the Coulomb penetration:

$$\frac{|\Psi_{\rm Coulomb}(r=0)|^2}{|\Psi_{\rm plane\ wave}(\text{large r})|^2} = F(Z,\epsilon) = \frac{2\pi\eta}{e^{2\pi\eta}-1}$$

$$\text{where}\ \ \eta = \frac{Z_1 Z_2 \alpha}{(v/c)} = \frac{-Z\alpha}{(v/c)}$$

We can estimate the average effect by using our Maxwell-Boltmann velocity distribution

$$\langle\frac{1}{v}\rangle = \int d\vec{v}\frac{1}{v}\left(\frac{m_e}{2\pi kT}\right)^{3/2} e^{-E/kT}$$

$$= \left(\frac{m_e}{2\pi kT}\right)^{3/2} 2\pi\int_0^\infty dv^2 e^{-E/kT}$$

$$= \sqrt{\frac{2m_e}{\pi kT}}$$

Now $2\pi\eta \sim -2.91$ at $T_7 \sim 1.5$. Thus to a good approximation we can replace $e^{2\pi\eta}-1$ in the denominator by an average value

$$|\Psi_{\rm solar}(r=0)|^2 \sim -1.06\ N_e 2\pi\eta \sim 1.06\ N_e 2\pi Z\alpha\sqrt{\frac{2m_e c^2}{\pi kT}}$$

So we have our answer

$$\omega^{\rm solar} = \omega^{\rm terrestrial}\left(\frac{\pi(\hbar c)^3}{2(Z\alpha m_e c^2)^3}\right)\left(2\pi Z\alpha 1.06\ N_e\sqrt{\frac{2m_e c^2}{\pi kT}}\right)$$

$$\sim \omega^{\rm terrestrial}\left(\frac{N_e}{3.5\cdot 10^{25}/{\rm cm}^3}\right)\frac{0.48}{T_7^{1/2}}$$

The normalizing density is typical of the center of the sun. If one uses a temperature of $T_7 = 1.5$, the above ratio is 0.4, which says that the electron density in hot solar core at the ^{7}Be nucleus is about 40% that in a cold terrestrial nucleus. As

$$\omega^{\rm terrestrial} = \frac{\ln 2}{53.29\ {\rm d}} \sim 1.50 \cdot 10^{-7}/{\rm sec}$$

$$\Rightarrow \omega^{\rm solar} = \frac{N_e}{3.5 \cdot 10^{25}/{\rm cm}^3} \frac{0.72 \cdot 10^{-7}/{\rm sec}}{T_7^{1/2}}$$

Again plugging in numbers, the above rate evaluated in the solar center corresponds to a ^{7}Be half life of 137 days, so a bit longer than the terrestrial half life.

Now the $^7{\rm Be} + p$ reaction comes right from our standard formula, which we write in terms of the rate per ^7Be nucleus

$$\omega_{17} = N_p(7.21 \cdot 10^{-19}{\rm cm}^3/{\rm sec}) \frac{1}{AZ_1Z_2} \frac{S_{17}(E_o)}{\rm kev - b} (Z_1^2 Z_2^2 A)^{2/3} \left(\frac{19.73}{T_7^{1/3}}\right)^2 e^{-(Z_1^2Z_2^2A)^{1/3}19.73/T_7^{1/3}}$$

$$= \frac{N_p}{3 \cdot 10^{25}/{\rm cm}^3} 1.4 \cdot 10^{10}/{\rm sec}\ e^{-47.6/T_7^{1/3}}\ T_7^{-2/3}\ S_{17}(E_o)$$

This S-factor has been the most controversial in the pp chain as the two best low-energy measurements disagreed by about 25%, an amount much larger than the claimed experimental uncertainties. But new measurements, especially one made at CENPA here at the UW, have yielded a more accurate value

$$S_{17} \sim .0207 \pm .0009\ {\rm keV - b}$$

is now favored. Plugging in

$$\omega_{17} = \frac{N_p}{3 \cdot 10^{25}/{\rm cm}^3} 2.9 \cdot 10^8/{\rm sec}\ e^{-47.6/T_7^{1/3}}\ T_7^{-2/3}$$

Thus

$$\frac{\omega_e(^7{\rm Be})}{\omega_p(^7{\rm Be})} = \left(\frac{N_e}{3.5 \cdot 10^{25}/{\rm cm}^3} / \frac{N_p}{3.0 \cdot 10^{25}/{\rm cm}^3}\right) 0.27 \cdot 10^{-15} T_7^{1/6} e^{47.6/T_7^{1/3}}$$

$$= \left[\begin{array}{ll} 7900 & T_7 = 1.2 \\ 330 & T_7 = 1.5 \end{array} \right]$$

Consistent with these number, when one averages over the solar core, one finds that 0.1% of the ^{7}Be burns by p + ^{7}Be, while the remainder is destroyed by electron capture.

Note also, however, that this branching ratio is quite sensitive to temperature. Figure 9 shows that the ppIII cycle can, indeed, becomes rapidly more important with increasing T, eventually dominating the pp cycle. Similarly, the temperature dependence determines the spatial region over which the various cycles are important in our sun.

ppI cycle strongest at low T $\Leftrightarrow$ burning occurs throughout the core
ppII cycle increases with T $\Leftrightarrow$ more important in central core
ppIII cycle increases fastest with T $\Leftrightarrow$ most important in very center

Finally, a byproduct of these reactions are the solar neutrinos. By incorporating the nuclear physics described above into the solar model, the following fluxes at earth are found (from Bahcall and Pinnsoneault 1995), in units of $\mathrm{cm}^{-2}\mathrm{s}^{-1}$

	E_ν^{max}(MeV)	Flux
$p + p \rightarrow d + e^+ + \nu_e$	0.42	$6.00E10$
$^8\mathrm{B} \rightarrow {}^8\mathrm{Be} + e^+ + \nu_e$	~ 15	$5.69E6$
$^7\mathrm{Be} + e^- \rightarrow {}^7\mathrm{Li} + \nu_e$	0.86(90%)	$4.89E9$
	0.38(10%)	
$p + e^- + p \rightarrow d + \nu_e$	1.44	$1.43E8$

4.6 CNO Cycles

Stars formed from the ashes of previous generations of stars will contain elements not produced in the big bang. As we have seen that charged particle reactions are suppressed by Coulomb barriers, the most interesting of these for helping to burn hydrogen at low temperatures are the lightest candidates. Carbon, nitrogen, and oxygen are the abundant, low Z, nonprimordial elements that one would first consider. These elements are produced by nuclear burning cycles in heavier stars and can be ejected into the interstellar medium through supernova explosions, stellar winds, etc.

In stars somewhat heavier than our sun, higher temperatures and densities are produced in the core when the star first achieves radiative equilibrium. If metals are present, hydrogen burning can be achieved more efficiently through the pp cycle by a faster process involving proton capture on heavier elements. The cycle that dominates at the lowest temperatures is

$$^{12}\mathrm{C} + p \rightarrow {}^{13}\mathrm{N} + \gamma$$

$$^{13}\mathrm{N} \rightarrow {}^{13}\mathrm{C} + e^+ + \nu_e \quad (\tau \sim 870\ s)$$

$$^{13}\mathrm{C} + p \rightarrow {}^{14}\mathrm{N} + \gamma$$

$$^{14}\mathrm{N} + p \rightarrow {}^{15}\mathrm{O} + \gamma$$

$$^{15}\mathrm{O} \rightarrow {}^{15}\mathrm{N} + e^+ + \nu_e \quad (\tau \sim 178\ s)$$

$$^{15}\mathrm{N} + p \rightarrow {}^{12}\mathrm{C} + {}^4\mathrm{He}$$

The important features of this cycle are

• It burns 4p $\rightarrow {}^4$He, just as the pp cycle does. The heavy nuclei are neither produced nor consumed. They are analogous to deuterium and ^{3}He in our pp discussion. But this CN cycle requires some initial concentration of the heavy elements to turn on. In this regard these metals are not like the pp cycle's d, ^{3}He.

• The cycle will clearly burn to equilibrium in the metals, which can affect the relative portions of the metals. But this is only a redistribution: no new heavy elements are created.
• The two β decay reactions are relatively fast. Thus when a temperature is reached where the proton capture reactions proceed readily, the cycle can be quite fast.

In our sun the total abundance by mass of elements with A greater than 5 is 0.02. With this significant metallicity, the CN cycle accounts for a nonneglible amount of the ^{4}He synthesis, somewhat less than 2%. Under similar conditions but with the temperature elevated to $T_7 \sim 1.8$, the CNO cycle would begin to overtake the pp chain in importance.

The fact that the CN cycle is taking over at $T_7 \sim 2.0$ means, in our sun, that one will not reach conditions where the ppIII cycle is primarily responsible for hydrogen burning.

The "cold" CN cycle reaction that is slowest is the $^{14}\mathrm{N}(p,\gamma)^{15}\mathrm{O}$ reaction. The comparative lifetimes for the various reactions are

$$\begin{array}{ll} ^{12}\mathrm{C}(p,\gamma)^{13}\mathrm{N} & 6.1\times10^{9}\mathrm{y} \\ ^{13}\mathrm{C}(p,\gamma)^{14}\mathrm{N} & 1.1\times10^{9}\mathrm{y} \\ ^{14}\mathrm{N}(p,\gamma)^{15}\mathrm{N} & 2.1\times10^{12}\mathrm{y} \\ ^{15}\mathrm{N}(p,\alpha)^{12}\mathrm{C} & 1.0\times10^{8}\mathrm{y} \end{array}$$

using the conditions $T_7 = 1$, $\rho = 100$ g/cm^3, and a hydrogen mass fraction of 0.5. Note (at this temperature!) that all of these lifetimes are much longer than the two weak lifetimes that play a role in the CN cycle. If the CN cycle is running in equilibrium, the production rate of each isotope must equal its destruction rate. It follows that the resulting equilibrium abundance of each isotope is inversely proportional to the rates above. For similar conditions but with a higher temperature ($T_7 = 5$), the relative abundances are

$$\begin{array}{ll} ^{12}\mathrm{C} & 0.055 \\ ^{13}\mathrm{C} & 0.009 \\ ^{14}\mathrm{N} & 0.936 \\ ^{15}\mathrm{N} & 0.00004 \end{array}$$

The large abundance of ^{14}N reflects its long lifetime.

The temperature dependence of energy production through the pp cycle is, at solar temperature, $\sim T^4$. Since the $^{14}\mathrm{N}(p,\gamma)$ is the controlling reaction for the CN cycle, we can plug into our rate formula to find out the temperature dependence of energy production through the CN cycle. The result is $\sim T^{17}$, much steeper. A graph of the competition between the pp and CNO cycles is shown in the figure.

The discussion above assumes that ^{15}N burns by the (p,α) reaction, but there is a competing possibility of $^{15}\mathrm{N}(p,\gamma)^{16}\mathrm{O}$ that leads to the CNO bi-cycle shown in the figure. Now the (p,α) reaction releases almost 5 MeV, which is nearly the height of the Coulomb barrier for

the outgoing channel. Thus the reaction is relatively insensitive to the outgoing Coulomb effects, and therefore ratio of these two reactions depends only on the S-factors (roughly). (The initial state penetration factor is common to both reactions.) This ratio for the (p, α) to (p, γ) reactions is 65 MeV-b to 64 keV-b, or about 1000. Thus the second cycle contributes only about 0.1% to the total rate of energy production.

There are further cycles, as indicated in the figure, involving reactions not all of which are definitely measured to the accuracy desired. There is a lot of activity in nuclear laboratories trying to improve the measurements.

The charge particle reactions of the CNO cycles increase in speed rapidly in temperature. If we use the estimate of T^{17} (see homework) and recall that the lifetime of ^{14}N at $T_7 = 1$ is 2.1×10^{12}y, we would conclude that it would live for about 660 s at $T_7 = 10$. Thus at such very high temperatures, the cycle time matches or exceeds the β decay lifetimes of ^{13}N and ^{15}O. Then it must be that the abundances of these isotopes become very significant. With all the proton capture reactions becoming fast at such temperatures, new cycles then open up, involving reactions like ^{13}N(p,γ)^{14}O. The CNO cycle operating above $T_7 = 10$ is called the hot CNO cycle. We will not continue the discussion any further, except to note that at temperature in excess of $T_7 \sim 50$, the rapid capture of protons may direct the nuclear flow outside of the hot CNO cycle, into heavier nuclei. The correct description of this physics requires simulations with large nuclear networks, and depends on some nuclear physics that is rather poorly known. This is also an interesting interface with stellar structure, as experts studying novae and other explosive environments have to specify what temperatures might be reached in order to access the probability of these rapid proton capture reactions.

4.7 Red giants and helium burning

We now consider the evolution off the main sequence of a solar-like star, with a mass above half a solar mass. As the hydrogen burning in the core progresses to the point that no more hydrogen is available, the stellar core consists of the ashes from this burning, ^{4}He. The star then goes through an interesting evolution:

• With no further means of producing energy, the core slowly contracts, thereby increasing in temperature as gravity does work on the core.

• Matter outside the core is still hydrogen rich, and can generate energy through hydrogen burning. Thus burning in this shell of material supports the outside layers of the star. Note as the core contracts, this matter outside the core also is pulled deeper into the gravitational potential. Furthermore, the shell H burning continually adds more mass to the core. This means the burning in the shell must intensify to generate the additional gas pressure to fight gravity. The shell also thickens as this happens, since more hydrogen is above the burning temperature.

• The resulting increasing gas pressure causes the outer envelope of the star to expand by a larger factor, up to a factor of 50. The increase in radius more than compensates for the increased internal energy generation, so that a cooler surface results. Thus the star reddens.

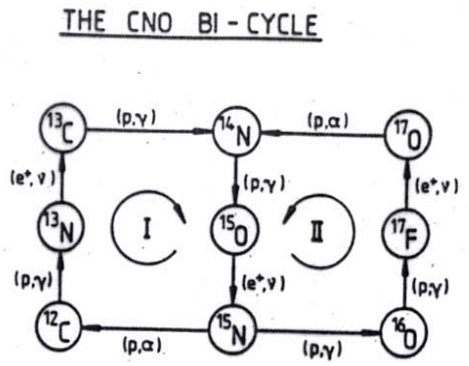

FIGURE 6.22. The interlocking sequence of reactions involved in hydrogen burning via the CNO bi-cycle. The burning of ^{17}O is assumed in this figure to proceed entirely by the $^{17}O(p, \alpha)^{14}N$ reaction.

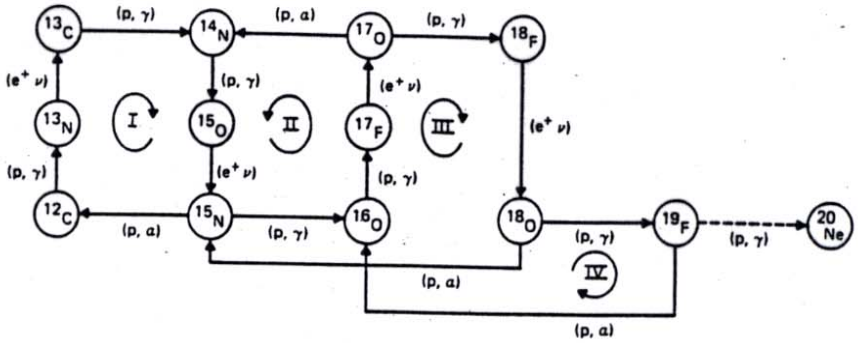

FIGURE 6.24. Illustration of the four CNO cycles involved in the conversion of hydrogen into helium. Catalytic material could be lost from the cycles via the $^{19}F(p, \gamma)^{20}Ne$ reaction, which would provide a link to the NeNa cycle (Fig. 6.27).

Figure 11: The CNO reaction cycle.

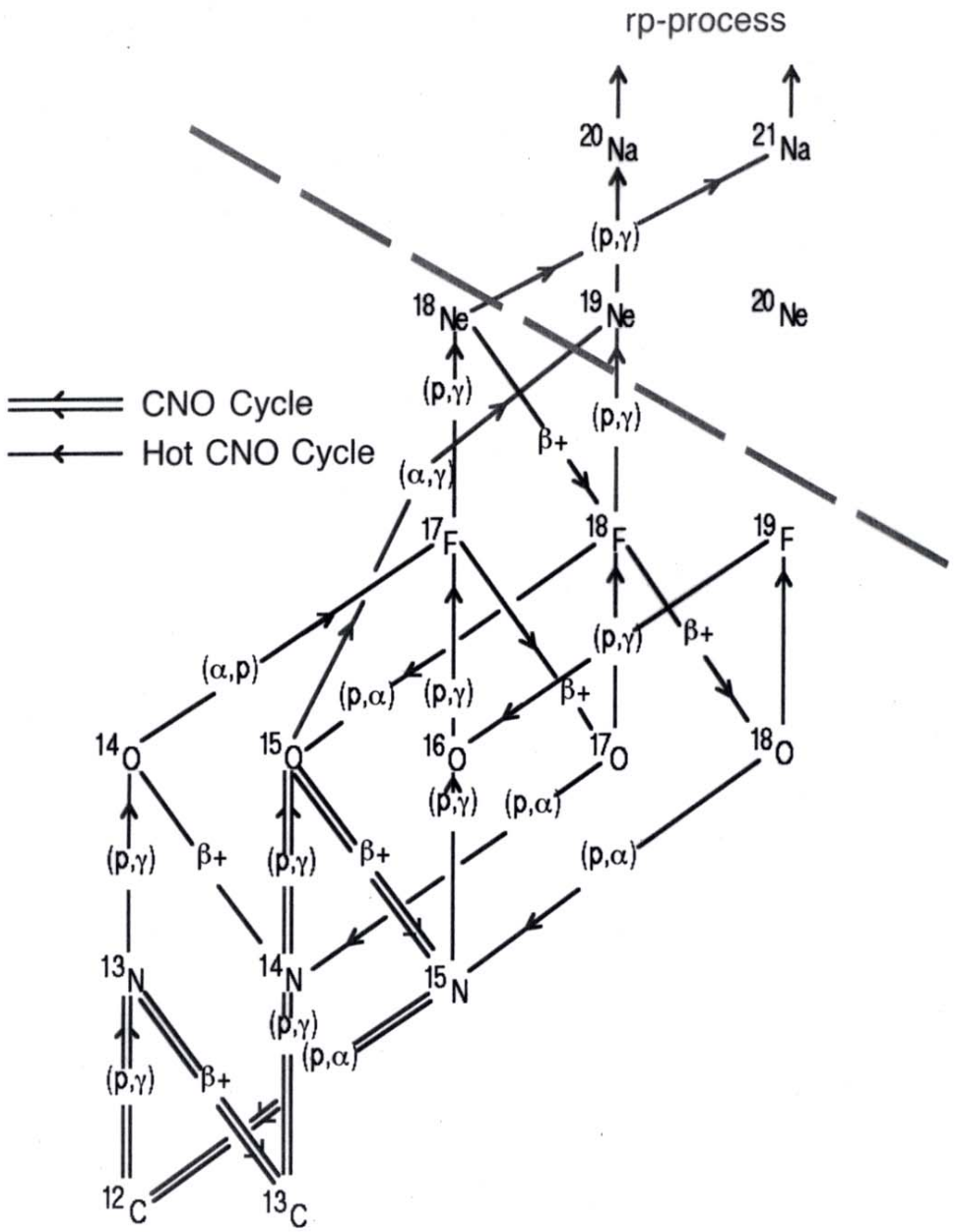

Figure 12: Another depiction of the CNO and hot CNO cycles.

Thus this class of star is named a red supergiant.
• This evolution is relatively rapid, perhaps a few hundred million years: the dense core requires large energy production and thus rapid evolution. The helium core is supported by its degeneracy pressure, and is characterized by densities $\sim 10^6$ g/cm^3. This stage ends when the core reaches densities and temperatures that allow helium burning through the reaction

$$\alpha + \alpha + \alpha \rightarrow {}^{12}\mathrm{C} + \gamma$$

This reaction is very temperature dependent

$$\propto \rho_\alpha^3 T^{30}$$

Thus the conditions for ignition are very sharply defined. That is, the core mass at this helium flash point is very well defined.
• The onset of helium burning produces a new source of support for the core. The energy release elevates the temperature and the core expands: He burning, not electron degeneracy, now supports the core. The burning shell and envelope have moved outward, higher in the gravitational potential. Thus shell hydrogen burning slows (the shell cools) because less gas pressure is needed to satisfy hydrostatic equilibrium. All of this means the evolution of the star has now slowed: the red giant moves along the "horizontal branch", as interior temperatures slowly elevate much as in the main sequence.

The 3α process depends on some rather interesting nuclear physics. The first interesting "accident" involves the near degeneracy of the ^{8}Be ground state and two separated αs: The ^{8}Be 0^+ ground state is just 92 keV above the 2α threshold. The measured width of the ^{8}Be ground state is 2.5 eV, which corresponds to a lifetime of

$$\tau_m \sim 2.6 \cdot 10^{-16}\mathrm{sec}$$

One can compare this number to the typical time for one α to pass another. The red giant core temperature is $T_7 \sim 10 \rightarrow E \sim 8.6$ keV. Thus v/c ~ 0.002. So the transit time is

$$\tau \sim \frac{d}{v} \sim \frac{5f}{0.002}\frac{1}{3 \cdot 10^{10}\mathrm{cm/sec}}\frac{10^{-13}\mathrm{cm}}{f} \sim 8 \cdot 10^{-21}\mathrm{sec}$$

This is more than five orders of magnitude shorter than τ_m above. Thus when a ^{8}Be nucleus is produced, it lives for a substantial time compared to this naive estimate.

This can be calculated from our resonant cross section formula.

$$\langle \sigma v \rangle = (\frac{2\pi}{\mu kT})^{3/2}\frac{\Gamma\Gamma}{\Gamma}e^{-E_r/kT}$$

where Γ is the 2α width of the ^{8}Be ground state. This is the flux-averaged cross section for the $\alpha + \alpha$ reaction to form the compound nucleus then decay by $\alpha + \alpha$. But since there is

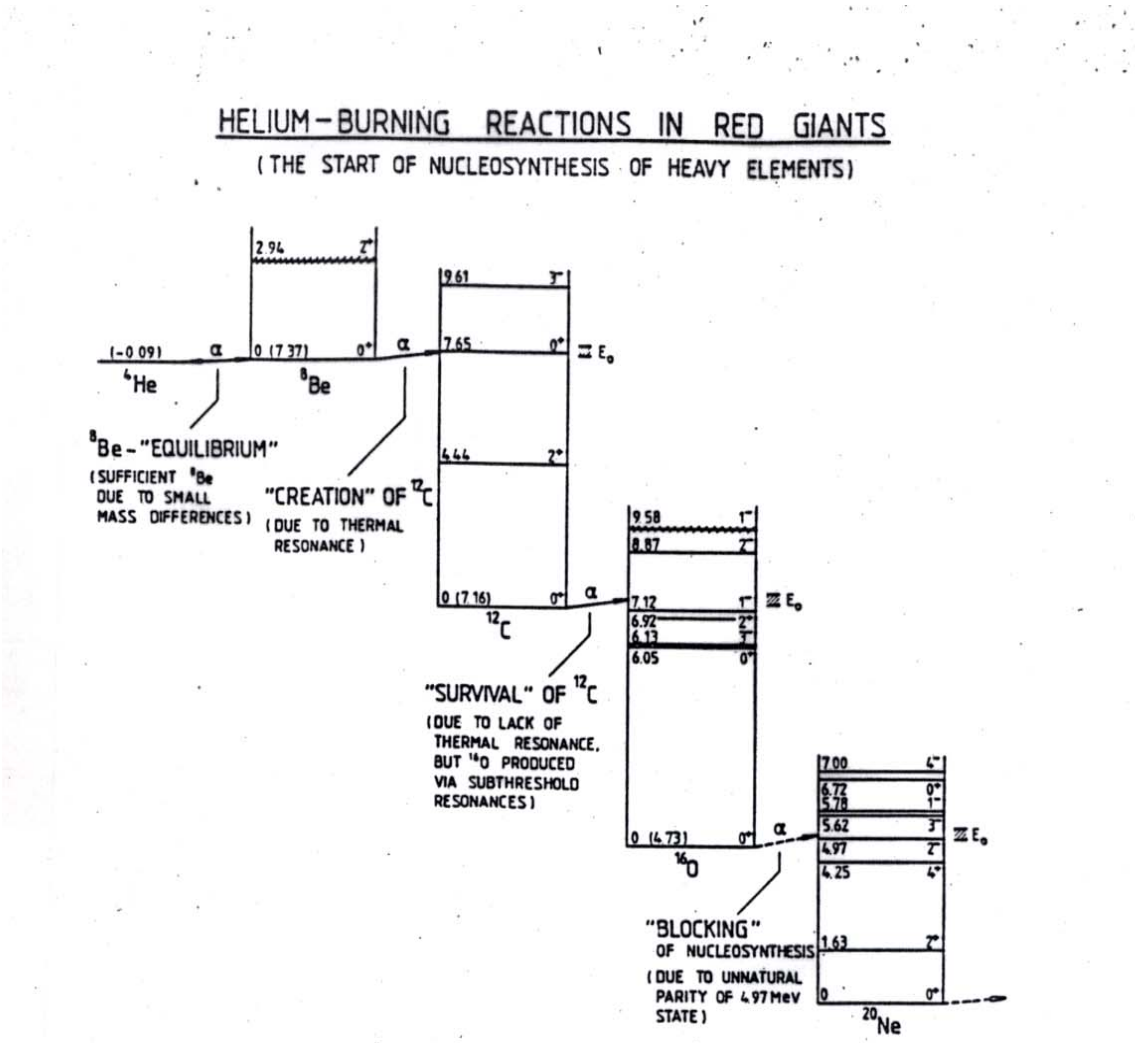

Figure 13: Level schemes of the nuclei involved in helium-burning reactions in red giants. Several nuclear structure coincidences – resonances with the right spins and parity existing at the required energies – allow stars to produce carbon and oxygen, elements important to life and major products of red giant evolution.

only one channel, this is clearly also the result for producing the compound nucleus ^{8}Be.

By multiplying the rate/volume for producing ^{8}Be by the lifetime of ^{8}Be, one gets the number of ^{8}Be nuclei per unit volume

$$N(\mathrm{Be}) = \frac{N_\alpha N_\alpha}{1+\delta_{\alpha\alpha}}\langle\sigma v\rangle\tau_m$$

$$= \frac{N_\alpha N_\alpha}{1+\delta_{\alpha\alpha}}\langle\sigma v\rangle\frac{1}{\Gamma}$$

$$= \frac{N_\alpha^2}{2}(\frac{2\pi}{\mu kT})^{3/2}e^{-E_r/kT}$$

Notice that the concentration is *independent* of Γ. So a small Γ is not the reason we obtain a substantial buildup of ^{8}Be. This is easily seen: if the width is small, then the production rate of ^{8}Be goes down, but the lifetime of the nucleus once it is produced is longer. The two effects cancel to give the same ^{8}Be concentration. One sees that the significant ^{8}Be concentration results from two efects: 1) $\alpha+\alpha$ is the only open channel and 2) the resonance energy is low enough that some small fraction of the $\alpha+\alpha$ reactions have the requisite energy. As $E_r = 92$ keV, $E_r/kT = 10.67/T_8$

$$N(\mathrm{Be}) = N_\alpha^2 T_8^{-3/2} e^{-10.67/T_8}(0.94\cdot 10^{-33}\mathrm{cm}^3)$$

So plugging in typical values of $N_\alpha \sim 1.5\cdot 10^{28}/\mathrm{cm}^3$ (corresponding to $\rho_\alpha \sim 10^5$ g/cm^3) and $T_8 \sim 1$ yields

$$\frac{N(^8\mathrm{Be})}{N(\alpha)} \sim 3.2\times 10^{-10}$$

Salpeter suggested that this concentration would then allow $\alpha+^8\mathrm{Be}\rightarrow^{12}\mathrm{C}$ to take place. Hoyle then argued that this reaction would not be fast enough to produce significant burning unless it was also resonant. Now the mass of ^{8}Be + α is 7.366 MeV, and each nucleus has $J^\pi = 0^+$. Thus s-wave capture would require a 0^+ resonance in ^{12}C at $\sim$ 7.4 MeV. No such state was then known, but a search by Cook, Fowler, Lauritsen, and Lauritsen revealed a 0^+ level at 7.644 MeV, with decay channels $^8\mathrm{Be}+\alpha$ and γ decay to the 2^+ 4.433 level in ^{12}C. The parameters are

$$\Gamma_\alpha \sim 8.9\mathrm{eV}$$

$$\Gamma_\gamma \sim 3.6\cdot 10^{-3}\mathrm{eV}$$

Our resonant cross section formula gives

$$r_{48} = N_8 N_\alpha (\frac{2\pi}{\mu kT})^{3/2}\frac{\Gamma_\alpha\Gamma_\gamma}{\Gamma}e^{-E_r/kT}$$

Plugging in our previous expression for $N(^8\mathrm{Be})$ yields

$$r_{48} = N_\alpha^3 T_8^{-3} e^{-42.9/T_8}(6.3\cdot 10^{-54}\mathrm{cm}^6/\mathrm{sec})$$

If we denote by $\omega_{3\alpha}$ the decay rate of an α in our plasma, then

$$\omega_{3\alpha} = 3N_\alpha^2 T_8^{-3} e^{-42.9/T_8}(6.3 \cdot 10^{-54}\mathrm{cm}^6/\mathrm{sec})$$

$$= (\frac{N_\alpha}{1.5 \cdot 10^{28}/\mathrm{cm}^3})^2 (4.3 \cdot 10^3/\mathrm{sec}) T_8^{-3} e^{-42.9/T_8}$$

Now the energy release per reaction is 7.27 MeV. Thus we can calculate the energy produced per gram, ϵ:

$$\epsilon = \omega_{3\alpha} \frac{7.27\mathrm{MeV}}{3} \frac{1.5 \cdot 10^{23}}{\mathrm{g}}$$

$$= (2.5 \cdot 10^{21}\mathrm{erg/g\ sec})(\frac{N_\alpha}{1.5 \cdot 10^{28}/\mathrm{cm}^3})^2 T_8^{-3} e^{-42.9/T_8}$$

We can evaluate this at a temperature of $T_8 \sim 1$ to find

$$\epsilon \sim (584\mathrm{ergs/g\ sec})(\frac{N_\alpha}{1.5 \cdot 10^{28}/\mathrm{cm}^3})^2$$

Typical values found in stellar calculations are in good agreement with this:

$$\text{red giant energy production} \Leftrightarrow 100\ \mathrm{ergs/g\ sec}$$

To get a feel for the temperature sensitivity of this process, we can do a Taylor series expansion

$$\epsilon(T) \sim T^{-3} e^{-42.9/T} \sim T_o^{-3} e^{-42.9/T_o} + (-3T_o^{-4} e^{-42.9/T_o} + T_o^{-3} e^{-42.9/T_o} (\frac{42.9}{T_o^2}))(T - T_o) + ...$$

$$= T_o^{-3} e^{-42.9/T_o} (1 + \frac{(T - T_o)}{T_o} \frac{42.9 - 3T_o}{T_o})$$

$$\sim T_o^{-3} e^{-42.9/T_o} (1 + \frac{T - T_o}{T_o})^{(42.9 - 3T_o)/T_o}$$

$$\sim \epsilon(T_o)(\frac{T}{T_o})^{(42.9 - 3T_o)/T_o}$$

That is

$$\epsilon(T) \sim (\frac{T}{T_o})^{40} N_\alpha^2$$

This steep temperature dependence is the reason the He flash is delicately dependent on conditions in the core.

3.11 Red giant burning and the neutrino magnetic moment

Prior to the helium flash, the degenerate He core radiates energy largely by neutrino pair emission. The process is the decay of a plasmon - which one can think of as a photon "dressed" by electron-hole excitations, thereby acquiring an effective mass of about 10 keV. The photon couples to a neutrino pair through a electron particle-hole pair that then decays

into a $Z_o \to \nu\bar{\nu}$.

If this cooling is somehow enhanced, the degenerate helium core would be kept cooler, and would not ignite at the normal time. Instead it would continue to grow until it overcame the enhanced cooling to reach, once again, the ignition temperature.

One possible mechanism for enhanced cooling is a neutrino magnetic moment. Then the plasmon could directly couple to a neutrino pair. The strength of this coupling would depend on the size of the magnetic moment.

A delay in the time of He ignition has several observable consequences, including changing the ratio of red giant to horizontal branch stars. Thus, using the standard theory of red giant evolution, investigators have attempted to determine what size of magnetic moment would produce unacceptable changes in the astronomy. The result is a limit on the neutrino magnetic moment of

$$\mu_{ij} \lesssim 3 \cdot 10^{-12} \text{electron Bohr magnetons}$$

This limit is more than two orders of magnitude more stringent than that from direct laboratory tests.

3.12 Carbon burning

The most abundant elements are H, He, C, and O, with the C/O ratio ~ 0.6. We have seen that the 3α process producing ^{12}C proceeds because of two fortuitous features of the nuclear physics: 1) there is a very small difference between the mass of two αs and ^{8}Be (recall the abundance of ^{8}Be depends on this mass difference); 2) there is a 0^+ resonance in ^{12}C that allows resonant capture of an α on ^{8}Be.

After ^{12}C is produced, one could imagine that additional α capture might be easier: there is a series of stable even Z-even N nuclei: ^{12}C, ^{16}O, ^{20}Ne, ... But there is an important question: is there a resonance in ^{16}O that might allow the synthesis to continue?

The structure of ^{16}O is shown in the figure. The mass of ^{12}C+α is 7.162 MeV. If we calculate the most effective energy E_o for this reaction at a temperature $T_8 \sim 2$, we obtain 300 keV. But there is no state in ^{16}O at 7.462 MeV: the nearest candidates are below threshold, a 1^- state at 7.12 MeV and a 2^+ state at 6.92 MeV. These states would allow ^{12}C+α to proceed by p-wave (E1) and d-wave (E2) capture.

This situation is very complicated, with interfering subthreshold resonances. Through a variety of measurements the S-factor as been estimated at 0.3 MeV-b. By our usual techniques one can calculate the reaction rate for a ^{12}C nucleus

$$\omega_{^{12}C} = (\frac{N_\alpha}{7.5 \cdot 10^{26}/\text{cm}^3}) 2.2 \cdot 10^{13}/\text{sec} \;\; e^{-69.3/T_8^{1/3}} T_8^{-2/3}$$

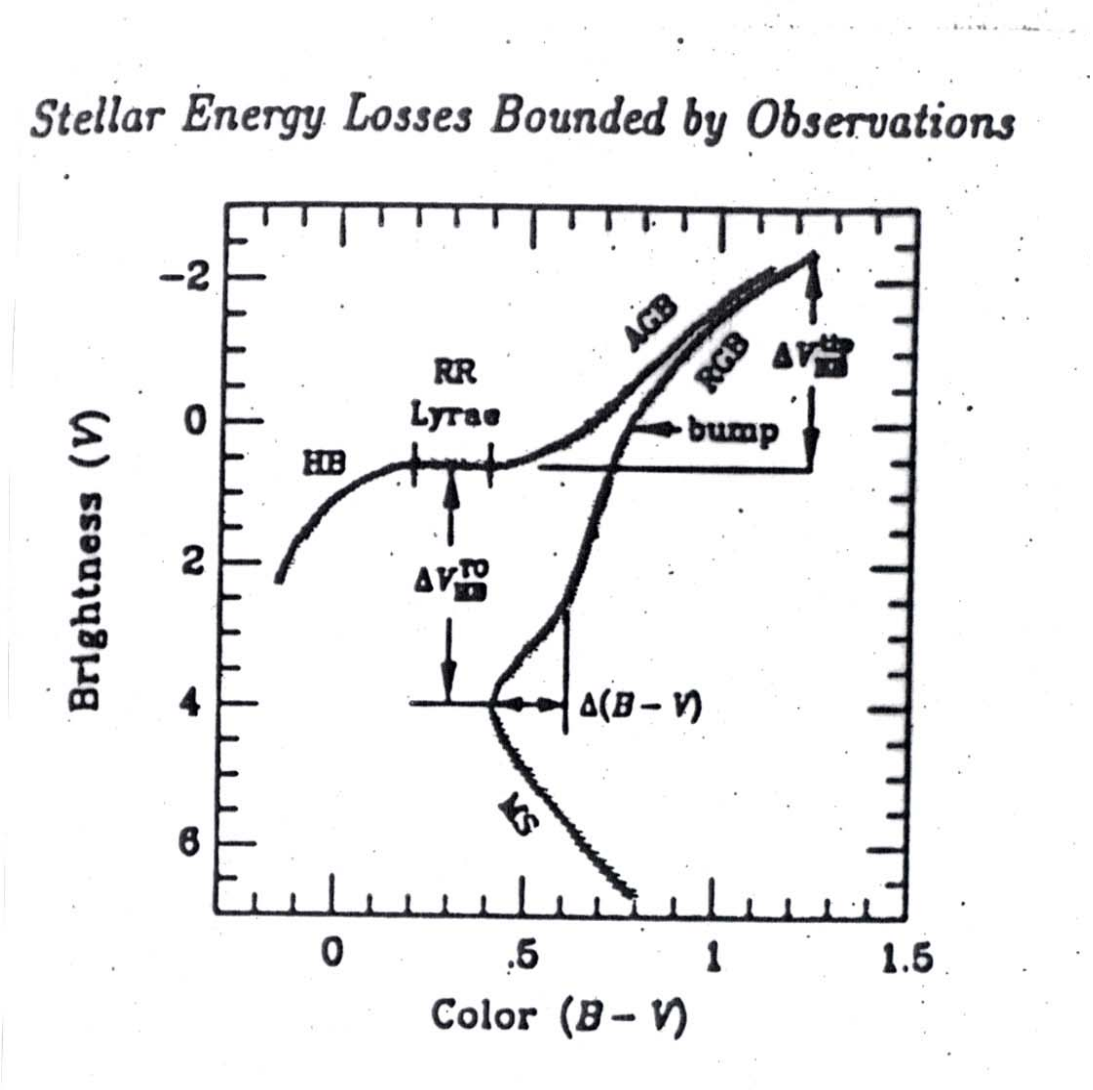

Figure 14: The HR diagram for red giant/horizontal branch star evolution. Various aspects of the red giant to horizontal branch evolutionary track provide constraints on anomalous cooling processes in red giants, such as enhanced neutrino production because of neutrino magnetic moments.

Note that $N_\alpha = 7.5 \cdot 10^{26}/\mathrm{cm}^3$ corresponds to a red giant density of 10^4 g/cm^3 and an α fraction of 0.5. Evaluating this yields

$$\omega_{^{12}\mathrm{C}} = \left(\frac{N_\alpha}{7.5 \cdot 10^{26}/\mathrm{cm}^3}\right) \left[\begin{array}{ll} 1.76 \cdot 10^{-17}/\mathrm{sec} & T_8 = 1 \\ 1.79 \cdot 10^{-11}/\mathrm{sec} & T_8 = 2 \end{array} \right]$$

These numbers correspond to ^{12}C lifetimes of $1.8 \cdot 10^9$ y and $1.8 \cdot 10^3$ y, respectively.

The net result is that the helium burning in a typical red giant is accompanied by relatively effective conversion of carbon to oxygen: the end ratio is about C/O ~ 0.1. (This number can vary a lot depending on the red giant mass: see Clayton. Note that Clayton's treatment is a little different from ours numerically.) Significant subsequent conversion of ^{16}O to ^{20}Ne does not occur because the 2^- resonance in Ne that is in the vicinity of the most effective energy has the wrong parity: since the α and ^{16}O have positive parity, L=2 capture produces a 2^+ state, not a 2^-. Thus the essential elements for life, carbon and oxygen, are the principle products of red giant burning.